On the Stability of Natural Circulation Loops with Phase Change

by

Troy C. Haskin

A preliminary report submitted in partial fulfillment of the requirements for the degree of

Doctor of Philosophy

Nuclear Engineering

at

University of Wisconsin–Madison

2012

Table of Contents

Table of Contents iii

List of Figures iv

List of Tables v

Nomenclature vi

1 Introduction 1

1.1 Research Purpose . . . 1

1.2 Reactor Cavity Cooling System . . . 1

1.2.1 Full-Scale System . . . 1

1.2.2 University of Wisconsin–Madison RCCS Experiment . . . 5

1.3 Literature . . . 10

1.3.1 Two-Phase Flow Instabilities . . . 10

1.3.2 Previous Analysis Efforts . . . 18

2 Theory 22

2.1 Conservation Laws of Thermal Hydraulics . . . 22

2.1.1 Single Phase . . . 24

2.1.2 Two-Phase . . . 26

2.2 Numerical Methods . . . 28

2.2.1 Spatial Discretization . . . 28

2.2.2 Time Discretization . . . 36

2.3 Stability Analysis . . . 38

3 Current Work **39**

3.1 Steady-state Solver 39

3.1.1 Description of the Algorithm 39

3.1.2 Test Problem 40

A Thermophysical Properties **42**

A.1 Equation of State 42

A.1.1 IAPWS Formulation 1995 42

A.1.2 Back Calculation of Temperature 44

A.2 Transport Properties 49

B Total Derivatives **50**

Bibliography **57**

List of Figures

1.1 ANL/UW-Madison water-cooled RCCS diagram 3
1.2 RCCS near-reactor-riser system 4
1.3 RCCS mass flow rate under blackout conditions 6
1.4 RCCS Experiment Full System diagram 7
1.5 RCCS Experiment Three Riser diagram 7
1.6 Mass flow rate versus time for the three riser tubes 9
1.7 Basic layout of the RCCS experiment 9
1.8 Ball-and-hill analogy of equilibrium descriptions 12

2.1 Geomtry to model 29
2.2 Acoustic speed versus material speed 37

3.1 A simple natural circulation loop 41

A.1 Pressure versus specific volume with several isotherms. The gray line denotes the phase coexistence curve. 45
A.2 Internal energy versus density with an arbitrary isochore 48

List of Tables

1.1 Summary of static flow instabilities 16

1.2 Summary of dynamic flow instabilities 16

1.3 Effects of parametric variation on instability 17

3.1 Comparison between the written steady-state solver and a hand calculation . 41

A.1 Select thermodynamic properties and associated dimensionless Helmholtz free energy relationships. 43

Nomenclature

Acronym

ANL	Argonne National Laboratory
HEM	homogeneous equilibrium model
IAPWS	International Association for the Properties of Water and Steam
RCCS	Reactor Cavity Cool System
NGNP	Next Generation Nuclear Plant
NRC	Nuclear Regulatory Commission

Greek

α_ϕ	Volume fraction of phase ϕ
β	Integral weight
Γ	Arbitrary, closed surface
ϕ	Arbitrary phase of fluid
ρ	Material density
Ω	Arbitrary, closed volume

Latin

c	Sound speed
i	Internal energy
$\mathbf{F}$	Vector-valued flux function
$g(z)$	Orientation specific gravitation acceleration
h	Enthalpy
K_{eff}	Effective frictional-and-form loss function
N	Semi discrete function/operator
P	Pressure
$\mathbf{q}$	Vector of conserved quantities
$\dot{Q}_{\text{add}}$	Heat addition function
$\mathbf{S}$	Vector-valued source function
T	Temperature
z	Primary spatial dimension

Subscripts

g	Gas phase of a fluid
ℓ	Liquid phase of a fluid

Chapter 1

Introduction

1.1 Research Purpose

The purpose of this research is to theoretically investigate the stability of a closed loop, natural circulation system with water as a working fluid. The motivations behind this research are given in the subsequent sections. The goal is to ultimately apply stability theory to three parallel channels in a closed circuit using various fluid models with a full equation of state for water. The literature review has found no application that uses this geometry with the intended level of modeling.

1.2 Reactor Cavity Cooling System

The primary motivation behind this stability work is the so-called Reactor Cavity Cool System (RCCS), which is a safety system for proposed Generation IV reactor designs. A definition and discussion of this safety system for full-scale application will be discussed first and followed by a description of an experimental test facility at the University of Wisconsin–Madison.

1.2.1 Full-Scale System

The Next Generation Nuclear Plant (NGNP) is a thermal-spectrum, gas-cooled reactor designed to be able to produce electricity as well as process heat for industrial applications.

A novel feature of the NGNP is the RCCS. The RCCS is a natural circulation system of ducts designed as the NGNP's ultimate heat sink for decay heat under a number of accident scenarios. There are two main designs under consideration which vary mostly in their working fluid: air-cooled and water-cooled. This work will focus on the water-cooled RCCS design, leaving air-cooled discussions left to the literature [4, 10]. A collaboration between Argonne National Laboratory (ANL) and the University of Wisconsin–Madison produced a base, full-scale RCCS system consisting of a two independent piping networks with each network having four main lines/tanks. Figure 1.1 outlines the basic design of system B but precludes any detail near the reactor. The elevation change of the system is on the order of several tens of meters with the reactor cavity portion being approximately twenty meters on its own. Within the reactor cavity, the eight cold lines of the RCCS splits into approximately 200 so-called riser pipes that line the cavity wall and ensconce the reactor (see figure 1.2). The riser pipes then receive heat from the uninsulated reactor pressure vessel via convection and radiation. Due to the heating, the fluid that fills the pipes is subjected to a buoyancy force that results in upward flow. During steady-state operation of the reactor, there is a persistent, parasitic heat loss from the reactor vessel to the RCCS of approximately 700 kW. If the reactor undergoes a loss-of-forced-flow accident with SCRAM, there is an expected peak decay heat load of 1.5 MW on the RCCS. If there is no loss of onsite or offsite power, the RCCS water storage tanks will be actively cooled, and the system is expected to maintain safe fuel temperatures for the duration of the accident. In the event of loss of onsite and offsite power (so-called station blackout), the RCCS can still continue to cool the reactor since the flow is naturally circulating, which is very important for the overall safety of the plant [34, §50.63].

However, without forced cooling, the reference temperature of the entire water system will continue to rise with continued decay heat exposure. At some point during the transient,

Figure 1.1: ANL/UW-Madison water-cooled RCCS diagram. Water flows from a tank, through the cold leg (blue), through the reactor cavity system, and through the hot leg (red) to some tank on the train at the same conditions (a closed circuit).

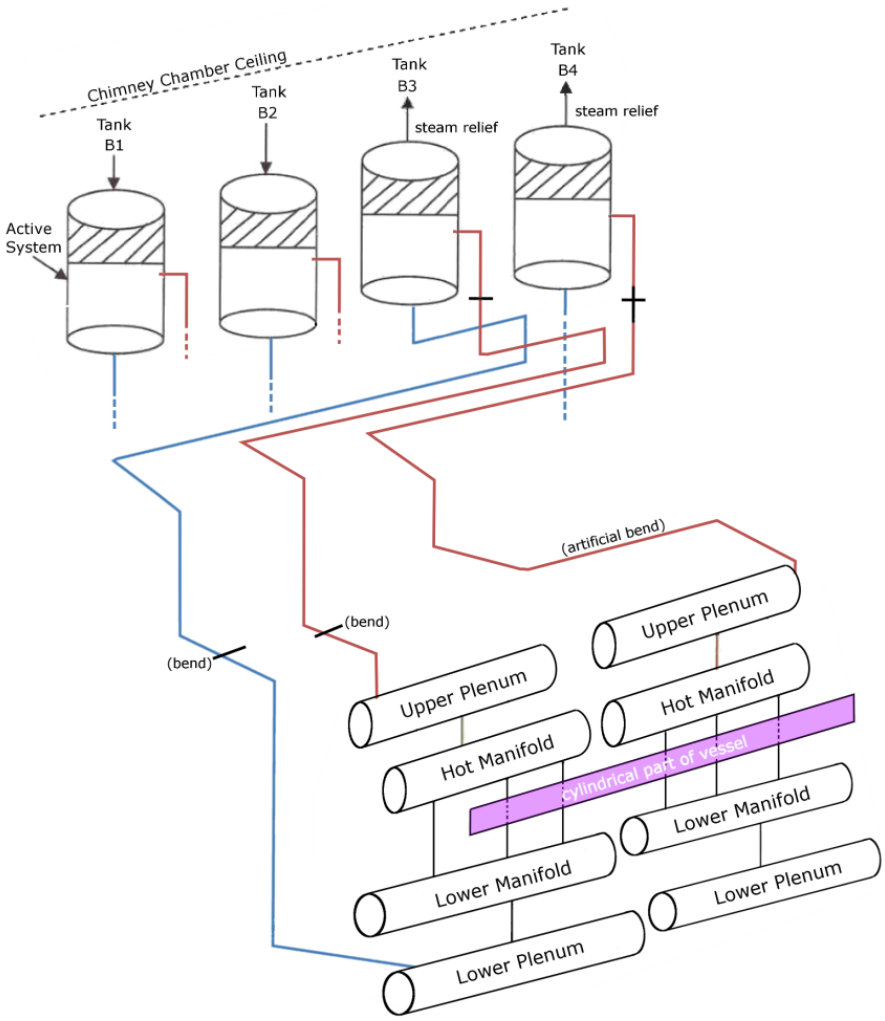

Figure 1.2: Cutaway picture of reactor vessel, RCCS ducts/pipes in the reactor cavity. The low temperature fluid is in blue and the high temperaure fluid is in red. The transparent boxes indicate network encasings. Credit: Darius Lisowski, University of Wisconsin–Madison.

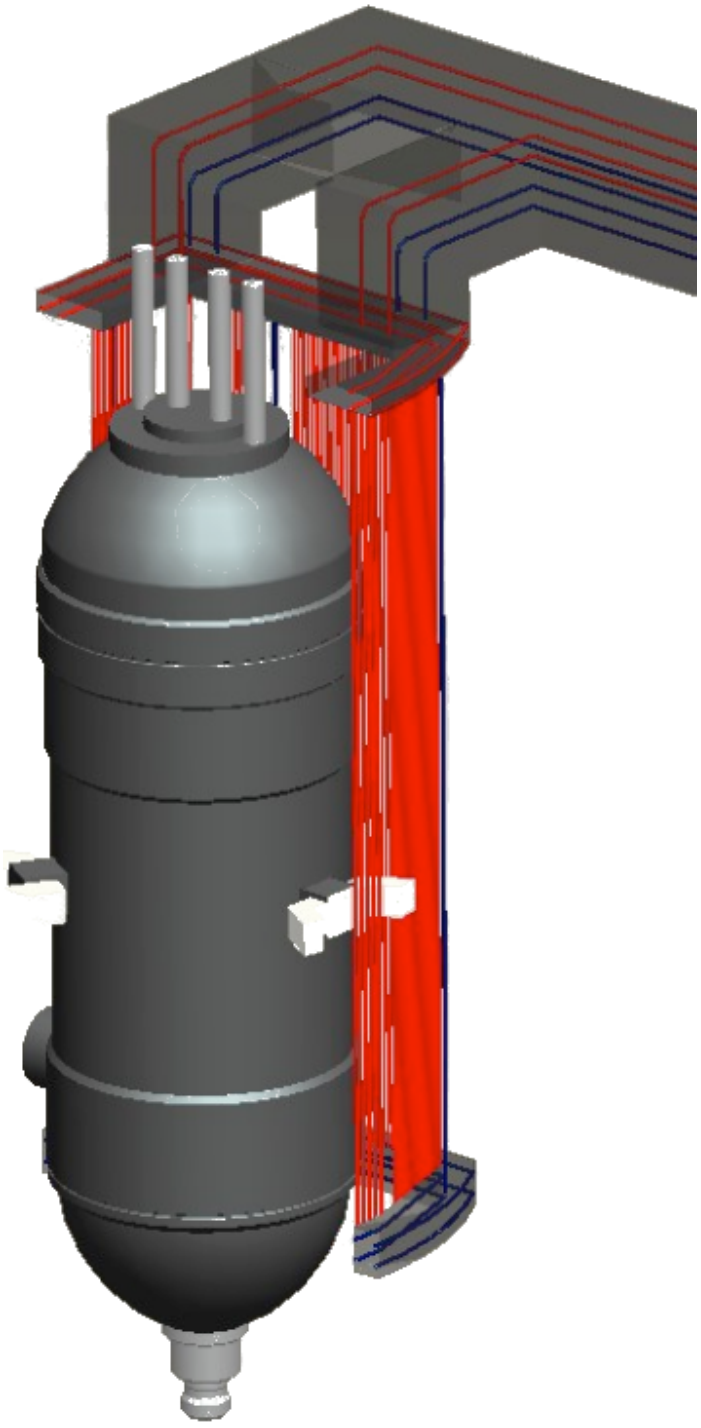

the water leaving the riser system will reach the saturation temperature at atmospheric pressure. Due to the gravitational head of all the water on top of the risers, the water will not immediately boil. Rather, as the water flows to the top of the system, it will instantly boil as it passes into a region where the ambient pressure is below the saturation pressure; this process is called flashing. This sudden, discontinuous jump in substance properties results in flow oscillations because the steam produced from the flash is approximately 1,000 times less dense (i.e., lighter) than the liquid state on the cold side of the system.

Figure 1.3 shows a numerical simulation of the full-scale system. Before flashing, the mass flow rate is increasing and non-oscillatory. At the onset of flashing, the flow rate rapidly oscillates and evolves in a complicated manner. At some point in the evolution, the system's flow rate stabilizes and evolves just as the single phase system. The period, amplitude, and overall time evolution of these oscillations is subject to numerous factors and various linear and nonlinear effects. The oscillations are commonly referred to as density wave instabilities since they are driven by the density of the system [1]. These incessant perturbations could potentially lead to large, erratic flow excursions that could pose a safety risk via extreme mechanical or thermal damage.

1.2.2 University of Wisconsin–Madison RCCS Experiment

Since the RCCS discussed above exists purely on paper, an experiment was built at the University of Wisconsin–Madison to directly observe and measure the behavior of an RCCS-like system. The experiment, presented in-brief by figure 1.4, is a scaled version of the full-scale RCCS in terms of both dimension and number of risers. While the full-scale system spans tens of meters with hundred of tubes, the experiment was scaled to a total height of approximately seven meters with three riser tubes. Heaters mounted opposite the riser tubes provide the power to drive the natural circulation of the system.

Figure 1.3: RCCS mass flow rate versus time under blackout conditions.

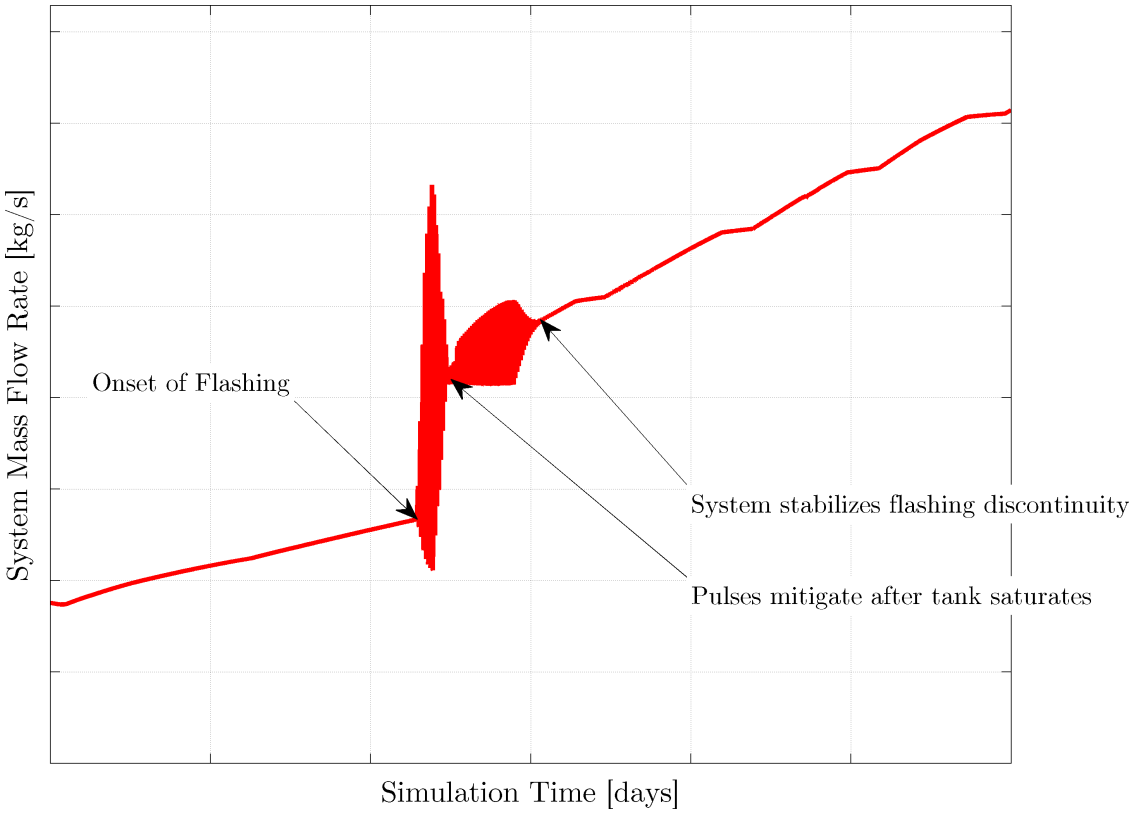

Figure 1.4: An overview of the whole RCCS experiment with important sections annotated.

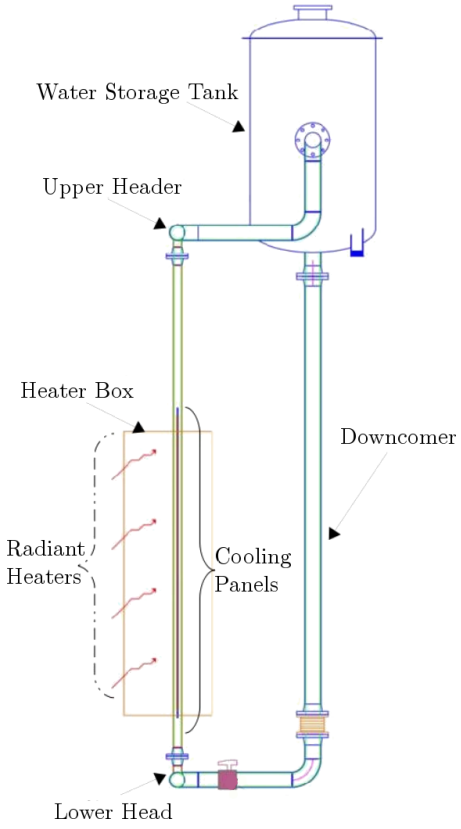

Figure 1.5: An overview of the RCCS experiment's three riser/radiant heater setup.

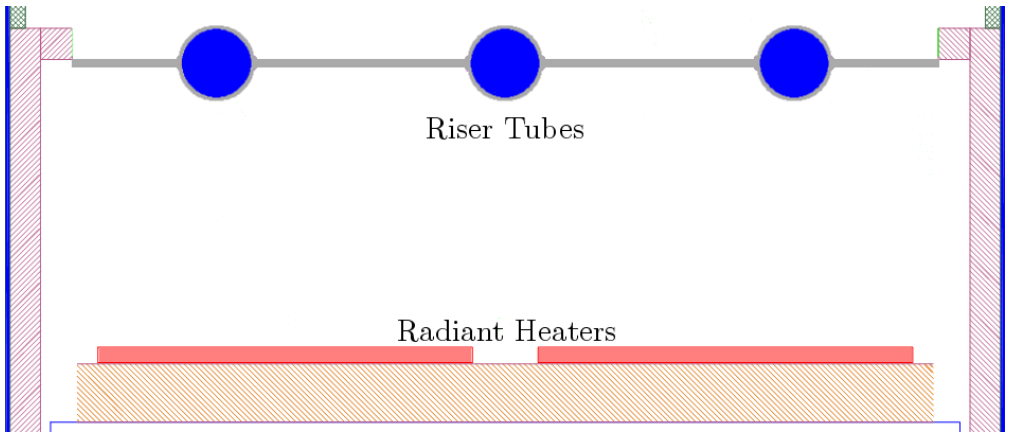

Due to the smaller scale and detailed design, a more precise numerical model could be made and benchmarked against data. The full convection/radiation enclosure for the heater box was used to simulate station blackout conditions as in the full-scale with a scaled heat flux. The mass flow rates from each of the risers for this accident simulation are shown in figure 1.6. The highly oscillatory nature of the flow rate after flashing begins is not only present but metastasized in this experiment. Additionally, reverse flows in two of the risers is present (though the total system mass flow rate is always positive). This local reversal of flow is more than likely systemic since short piping at the top allows a two-phase condition to exist at the top of the red riser. While not expected in the full-scale system, this flow reversal is an interesting feature of the experiment's design and should be investigated.

Figure 1.6: Mass flow rate versus time for the three riser tubes of the RCCS experiment with station blackout accident conditions. The colors of the plot lines correspond to the riser colors in figure 1.7.

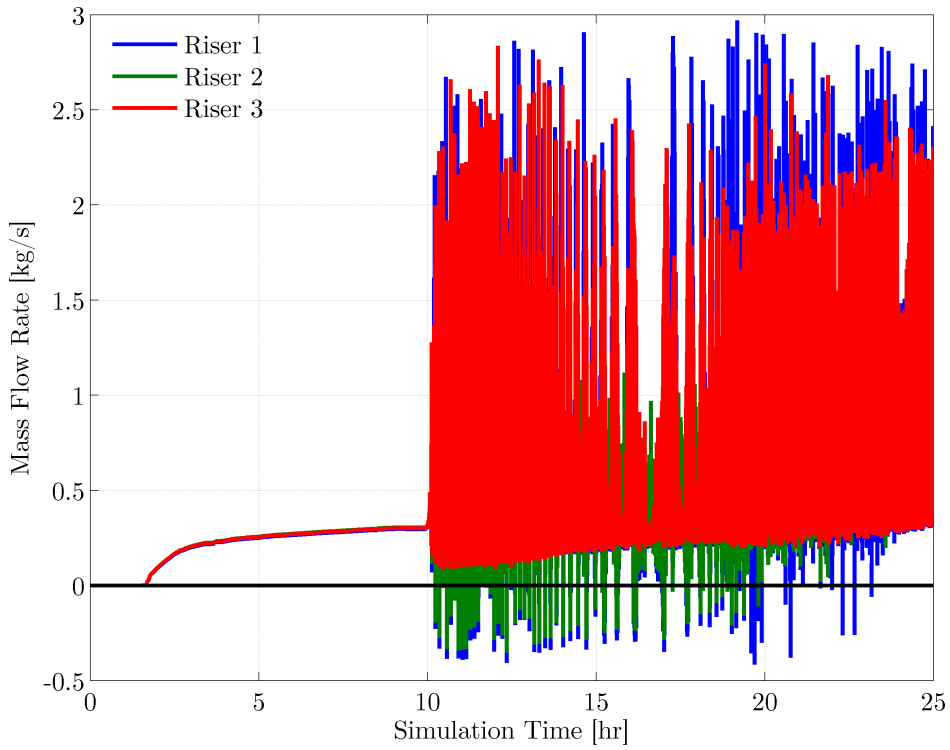

Figure 1.7: Basic layout of the RCCS experiment's numerical model. The blue and red outlines denote the cooling and heating zones, respectively.

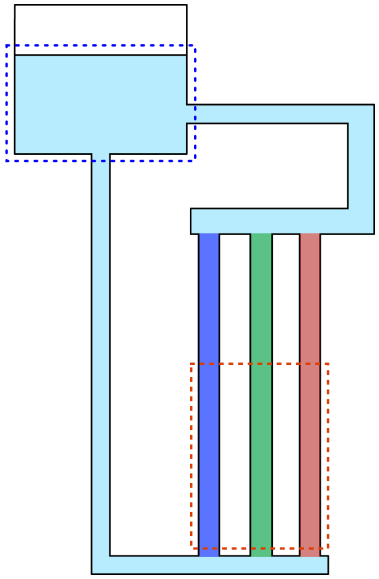

1.3 Literature

Two-phase flow instabilities have been extensively studied for numerous industrial applications, including thermosiphons and power cycle loops. Therefore, the literature of two-phase flow instabilities is extensive. It should be noted that single phase instabilities do exist and are researched [36], but an in-depth overview of those mechanisms will not be given. As such, an overview of two-phase instabilities, classifications, and definitions will be given. Then, specific discussion of efforts and techniques in the analysis will be discussed.

1.3.1 Two-Phase Flow Instabilities

There are a variety of ways to classify two-phase flow instabilities depending on geometry, spatial/temporal dependence, multiphase models, etc. Difficulties also arise when real world applications see a convergence of all of these parameters. Both Boure et al. and Kakac et al. provide extensive discussions of general two-phase flow instability characterization [6, 21], and their similar systems for describing two-phase will be used throughout this section. Tables 1.1 and 1.2 present a summary of general two-phase instabilities presented by the above authors; however, not all of them will be discussed in detail. Presad et al. [9] and Nayak et al. [32], while overlapping somewhat with the generic descriptions of instabilities, present and classify certain instabilities as natural circulation specific that should be described. Most of the following discussion concerns a flowing fluid undergoing phase transition in a channel which may require some familiarity with two-phase flow regimes; explanation of these regimes is left to the literature (e.g. [38, 39, 11]).

For clarity, key terms will be defined. If a system at steady-state is perturbed and eventually returns to its initial equilibrium, the system is described as stable. If a system at steady-state is perturbed into a neighborhood where no equilibrium exists near the initial state,

the system possesses a static instability. A system has dynamic instabilities if there are inherently transient feedback mechanisms that may lead to a steady-state, though there is no guarantee of uniqueness. An instability that arises from another is referred to as a secondary phenomenon (the instigator being the primary). A compound instability is one that incorporates two or more mechanisms that confound analysis; fundamental instabilities are the opposite. Using a standard physical analogy, figure 1.8c is a stable system while figure 1.8d is an example of a system with a static instability.

One aspect of the stability the above definitions do not discuss is the magnitude of the system perturbations. The strength of the perturbation is important since it determines how much energy is imparted into the system and, therefore, how far the system will travel from its initial state. The importance can be seen in figures 1.8e and 1.8f where both systems exhibit different behavior depending how hard the system is "hit." Figure 1.8e shows a linear instability while actually being nonlinearly stable with multiple equilibria. Figure 1.8f exhibits linear stability while being nonliearly stable These concepts are important to consider when looking at linear stability because the behavior beyond the system's linear boundary is technically *terra incognita*. Actually performing a nonlinear analysis, if possible, is the only surefire tool for assessing stability.

Static Instabilities

Static instabilities are characterized by either a pure steady-state analysis or an analysis that foresees dynamic feedback from the steady-state system. The analysis tools used to derive stability boundaries for these instabilities will be discussed in section 2.3.

A flow excursion, also known as a Ledinegg instability, is the sudden drop in a steady flow rate to a lower, steady value. This jump occurs when the pressure losses in a system decrease with

Figure 1.8: Ball-and-hill analogy of equilibrium descriptions. The ball represents some state at a given time and place, and the shapes supporting the ball dictate how the state moves when subjected to a perturbation. Troughs are considered stable while crests/runoffs are unstable.

(a) Neutral equilibrium (infinitely many steady-states)

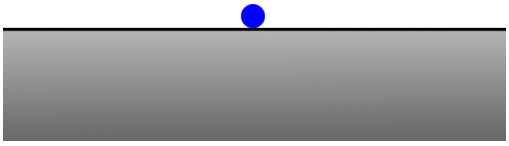

(b) No equilibrium (no steady-state)

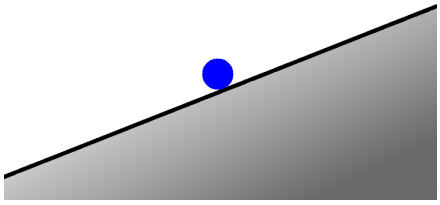

(c) Stable equilibrium

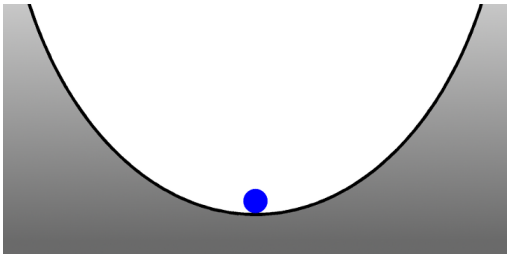

(d) Unstable equilibrium

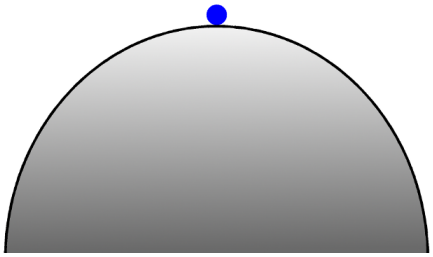

(e) Linearly unstable, nonlinearly stable equilibrium

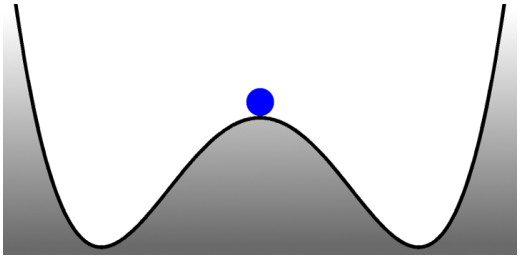

(f) Linearly stable, nonlinearly unstable equilibrium

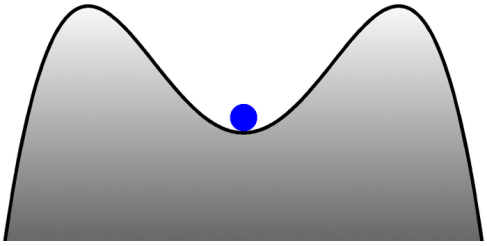

increasing flow rate. For a liquid undergoing phase change in a channel, there is a complex, internal relationship between the buoyancy, friction, and acceleration momentum terms that must be taken into account for steady flow. If the flow is forced by external sources and the internal forces of the flow are not properly taken into account, then the pressure drop could rise with increasing flow; this is especially true for slightly sub-cooled flows entering a heated region where a sudden change in void fraction can have a large impact on the flow behavior with the system.

Fundamental relaxation instabilities occur when two or more flow regimes have state equilibriums close to each other. For example, a bubbly flow that experiences a small change in flow rate could transition to the annular regime. Then, the flow rate will experience an increase since annular flow has a relatively low pressure drop, and the flow regime transitions back to the bubbly regime. Given the right situation, this cycle could continue ad infinitum. The flow regime transitions act as a relaxation mechanism (in the dynamical system sense) that causes persistent, periodic behavior.

Chugging is an instability associated with the jetting of large vapor structures from a flow channel into larger space. This instability typically occurs with low velocities and moderate void fractions [39]. A flowing liquid receiving heat may development large vapor bubbles in a coolant channel; this increases the flow rate due to the vapor-to-liquid ratio. After the bubbles have been expelled, and possibly quenched, at the channel exit, the flow rate will return to the pre-slug rate. As with the relaxation instability, this mechanism also has a periodic nature [2].

Dynamic Instabilities

Dynamic instabilities, unlike static, are inherently transient and primarily involve the transmission of information via waves. As is discussed further in chapter 2, thermal hydraulic systems typically possess a material (or density) wave and an acoustic (or pressure) wave. For a non-ideal fluid, the acoustic wave's speed is primarily a function of the system's density and temperature while the material wave travels near the physical speed of the system.

Acoustic instabilities are typically of high frequency (10Hz–10kHz) and have been observed in various boiling regimes. The acoustic waves were found to cause large pressure drop oscillations relative to steady-state values. Even in situations where the lower frequency density waves were present, there was a clear superposition of high frequency acoustic waves with the material waves. At high pressure-and-temperature water experiments, the acoustic waves reached frequencies that were clearly audible (so-called whistler modes).

Material wave instabilities are the most common in two-phase flow and are a highly physical phenomenon that occur from a complex coupling of thermal hydraulic equations, constitutive relations, and geometry. These waves have also been described as "flow-void feedback instabilities" for boiling systems [33] and "time-delay oscillations" due to the relatively slow transmission of information at material speed [5]. Since the oscillation has its roots in the differing densities of a fluid's liquid and gas phases, vertical channel height (where the system pressure changes greatly with position), inlet conditions (thermodynamic and kinematic), and total heat transfer between the fluid and the surroundings are extremely important in the control and appearance of these flow oscillations. It has been found that by increasing the system pressure these oscillations can be mitigated or eliminated since the density ratio of the competing phases approach one another as the pressure increases.

These material oscillations can lead to oscillations in the boiling heat transfer processes at

the wall and results in a compound thermal instability. The emphasis here is put on the highly variable nature of the two-phase heat transfer coefficient at the wall and how the information being propagated from the wall interacts with material wave oscillations. The effects of this interaction can be as bad as an oscillating dry point in the channel with large temperature oscillations.

Natural Circulation Instabilities

There are two natural circulation instabilities of primary interest: flashing and compound natural circulation. As mentioned in section 1.2, flashing occurs when a high temperature liquid flows into a region of lower pressure such that it enters a saturated or superheated state and immediately bursts into a two-phase mixture. This mechanism is a primary cause of material wave instabilities in natural circulation loops at low pressures or long vertical channels. This type of instability is currently under examination for one and two protypic fuel channels [27, 28].

The final instability is the compound natural circulation instability. This instability is the confluence of vertical channel heating, material wave oscillations (possibly due to flashing), chugging phenomenon, and flow regime transitions. Since the system's flow rate is not subject to any mechanical head contributions, all of these instabilities can occur concurrently and must be carefully analyzed to discern which of the mechanisms are present and which is dominate. These instabilities are extremely important for all types of nuclear reactors and are under continuously under investigation [7, 3, 42].

Table 1.1: Summary of static flow instabilities due to [6]

Name	Class	Mechanism	Characteristics
Flow excursion	Fundamental	$\frac{\partial \Delta P}{\partial(\rho u)}\big\|_{\text{int}} \leq \frac{\partial \Delta P}{\partial(\rho u)}\big\|_{\text{ext}}$	Sudden, large flow change to a new, stable state
Boiling crisis	Fundamental	Ineffective cooling	Wall temperature excursion and flow oscillation
Flow Regime Transition	Fundamental Relaxation	Varying ΔP between regimes	Cyclic flow pattern transitions and flow rate variations
Bumping, geysering, or chugging	Compound Relaxation	Periodic adjustment of metastable conditions	Periodic superheat and violent evaporation

Table 1.2: Summary of dynamic flow instabilities due to [6]

Name	Class	Mechanism	Characteristics
Acoustic Oscillations	Fundamental	Resonance of pressure waves	High frequency oscillations near the acoustic speeds
Density Wave Oscillations	Fundamental	Coupled mass, momentum, and energy feedback	Low frequency oscillations near the material speed
Thermal Oscillations	Compound	Variable heat transfer coefficient interacting with flow	Occurs during film boiling
BWR Instability	Compound	Hydraulic-neutronic coupling	Strong only for a small fuel time constant and low pressure
Parallel Channel Instability	Compound	Interaction among parallel channels	Various modes of flow redistribution
Pressure drop Oscillations	Secondary Compound	Flow excursions initiate interactions between channels and compressible volumes	Very low frequency, periodic process

Table 1.3: Effects of parametric variation on instability for a flow entering a vertical channel sub-cooled or saturated due to [9]

Parameter Increased	**Effect**	**Reason**
System pressure	Stability increases	Phase density difference lessens thus reducing the gravitational head gain.
Mass flow rate	Stability increases	Critical power for oscillation generation increases and avoids chugging.
Inlet sub-cooling	Destabilizes at small sub-coolings but stabilizes otherwise	For small sub-coolings,due to significant response delay in void formation with an increase in transit time. Otherwise, it reduces void fraction and increases non-boiling length.
Inlet resistance	Stability increases	Increases the single phase friction which has a damping effect upstream.
Exist resistance	Stability reduces	Increases two-phase friction which amplifies instabilities upstream
Riser height	Stability reduces	Increases two-phase gravitational pressure drop and phase transition as static head decreases

1.3.2 Previous Analysis Efforts

The two main types of analysis employed in stability analysis are linear and nonlinear (nonlinear being a superset of the other). Every analysis begins with a defined set of the conservation/balance equations. These equations possess all of the modeling information and assumptions in the analysis to be performed. Three commonly used models are [20]:

- a homogeneous equilibrium model (HEM) where the distinct phases of a boiling fluid are treated as a single fluid with averaged properties;
- a separated flow model (SFM) where an additional momentum equation is added to the HEM allowing phase slip;
- a two-fluid model where the distinct phases are treated as separate partitions of a total volume, have completely separate properties, and only communicate through their shared interface.

Chapter 2 discusses the HEM and two-fluid equations, but for now, it suffices to say that these equations are nonlinear, coupled partial differentials equations that do not, in general, admit analytical solutions.

After the model has been decided, authors either linearize the equations or not and assess the system's stability through various techniques. The specifics of the solution techniques are left to section 2.3 since the techniques are all similar. What makes the approaches more interesting is the models used, approximations made, and geometry considered.

Wallis and Heasley present one of the earliest efforts to analytically tackle two-phase flow oscillations [40]. They investigated a simple, closed natural circulation loop with pentane as the working fluid. The analysis method looked at three sources of oscillations from a

Lagrangian frame. The first source was changes in riser buoyancy resulting from velocity perturbations and an equation for the marginal stability was derived in terms of the friction factor's derivative with respect to some steady-state velocity. The second source was the heat input into the system with a theorized flow excursion for their loop. Lastly, they investigated parallel channels but did not complete the analysis due to the then intractability of the solution.

Welander, though not a study of two-phase instabilities, investigates a simple, closed loop with point sources and proportional constitutive relations.[41]. While the treatment is similar to Wallis and Heasley's, Welander's more mathematical approach is more in-line with this work's goals. Additionally, Welander derived an asymptotic steady-state solution and also compared the analytical neutral boundary with numerical experiments to confirm the boundary's validity. Zvirin and Greif continued this work by examining how an arbitrary initial condition evolved toward Welander's steady state [43]. They found that while the solution approached the analytical steady-state, the solution was without oscillation and concluded that the oscillation characteristics were strongly dependent on the shape of the initial condition.

Achard et al. investigated material wave oscillations in a horizontal boiling channel using both linear and nonlinear analysis [1]. They derived a lumped parameter integrodifferential equation. Upon linearizing the equation and using the friction and sub-cooling numbers as degrees of freedom, they found two absolutely unstable regions, several conditionally unstable regions, and one absolutely stable region. The conditionally unstable regions were found to depend on how actual system's state evolved in time and moved through the stability space. They also performed a nonlinear analysis where the parameter values to maintain stability were obtained by nonlinearly solving the lumped parameter equation for a given perturbation amplitude. The nonlinear analysis showed that stable parameter curves existed for their

system but the absolutely stable region shrank with increasing perturbation amplitude.

Lee and Ishii performed a linear analysis similar to Welander, but the system was explicitly two-phase, had a quadratic frictional dependence in velocity with a constant friction factor, and had a distributed heat load [24]. Additionally, as an extension of the Zvirin and Greif's methodology, Lee and Ishii divided the loop into size different regions with average properties and solved for the stability boundary using linear analysis.

Lee and Lee performed nearly the same analysis as Lee and Ishii with the added difficulty of a variable, flow-regime dependent friction factor [25]. Guanghui et al. also performed a similar analysis over a simple, closed loop that compared very well experiments [15].

Knaani and Zvirin investigated the existence of multiple steady-states for a simple, closed loop undergoing boiling[22]. The analysis was done with HEM and incorporated a guess and check procedure for finding a solution to the nonlinear problem. They ultimately found multiple steady-states for the closed system due to the non-monotonic nature of the buoyancy term during phase change. Nayak et al. also performed analysis on a simple, closed loop but used a four equation model (two for mass and mixture equations for energy and momentum) and several different two-phase friction multipliers [31].

Lee and Pan undertook an homogeneous equilibrium model (HEM) for a two-phase natural circulation system with two parallel, heated channels [23]. This treatment is the first work in this review to explicitly analyze a non-simple closed loop. Through a number of piece-wise integrations along the loop, the authors arrived at a set of ordinary differential equations that satisfied the zero pressure gradient requirement of the closed loop. Using the channel inlet sub-cooling as a parametric and a blackbox solver, the authors compared the steady-state channel flow rates with experimental data. The authors then found a stability curve for even heating of the channels that possessed two unstable regions and one stable region.

The author concluded with a parametric study of how the stability region shifted with the addition of an orifice plate.

Chapter 2

Theory

In this chapter, the underlying theory of the previous chapter is explained. Basic conservation laws for thermal hydraulics are presented for both single and two-phase flow in one-spatial direction. The numerical solution of these laws is then discussed. Concluding the chapter, an overview of stability analysis of systems is given.

2.1 Conservation Laws of Thermal Hydraulics

In general, conservation laws are a set of nonlinear, partial differential equations of mixed character. For a one-spatial dimension formulation, as will be used throughout this work, the equations can be succinctly described as balance laws that have a dominant hyperbolic character (meaning the information travels is a particular direction at a finite speed). In general, for a vector of variables $\mathbf{q}$ that are conserved in one dimension, a nonlinear set of conservation laws has the form

$$\frac{\partial \mathbf{q}}{\partial t} + \frac{\partial \mathbf{F}(\mathbf{q}; z, t)}{\partial z} = \mathbf{S}(\mathbf{q}, z, t), \tag{2.1}$$

where $\mathbf{F}(\mathbf{q}; z, t)$ is referred to as the flux function of $\mathbf{q}$ and $\mathbf{S}(\mathbf{q}, z, t)$ is the source function of $\mathbf{q}$. The particular form of the flux and source functions depends on the particular model being used. However in the above equation, it is assumed that all explicitly first-order derivatives are represented by the gradient of the flux function, and the source function may possess derivatives of higher degree.

An important feature of equation 2.1 is that the flux function is directly dependent only on $\mathbf{q}$ (parametrized by z and t). Therefore, it can written in a quasilinear form

$$\frac{\partial \mathbf{q}}{\partial t} + \frac{\partial \mathbf{F}(\mathbf{q}; z, t)}{\partial \mathbf{q}} \frac{\partial \mathbf{q}(z, t)}{\partial z} = \mathbf{S}(\mathbf{q}, z, t), \tag{2.2}$$

where the chain rule allowed the gradient of the flux function to be transformed into the flux function's Jacobian times the conserved variables's gradient. Although, this form is not used in the numerics of this work, it is important to mention two features of this form [26]:

1. the eigenvalues of the Jacobian matrix yield the speeds at which information propagates through the system.
2. equation 2.1 is said to be hyperbolic if the flux function's Jacobian is diagonalizable with purely real eigenvalues.

One set of fundamental equations for thermal hydraulics is the conservation of mass, momentum, and energy system. In this system, the same set of three equations are used to evolve a predefined fluid. For simulations that involve multiple fluids, a set of three equations is needed for either each fluid or for a grouping of fluids, which is called a field. For example, MELCOR, a safety analysis program used by the Nuclear Regulatory Commission (NRC), has two fields: pool and atmosphere. The pool contains and evolves all information about liquid water and entrained droplets, and the atmosphere contains and evolves all information about water vapor and noncondensible gases [35].

Throughout this section, when discussing a particular conservation law, the conserved quantities are those which appear under the time derivative of the system (cf. equation 2.1). As such, when the so-called primitive variables (as opposed to conserved variables) of velocity u and internal energy i always appear with a preceding ρ (i.e., ρu and ρi), they are to be regarded as an unbreakable quantity. However, sometimes for ease of reading, equations will

be put into primitive variables.

2.1.1 Single Phase

The simple starting point for discussing specific conservation laws is a single phase, one field formulation. A thorough derivation of all three equations for a single phase fluid is presented by Mills [29, pg. 451]. The three conserved variables are the density ρ, momentum ρu, and internal energy ρi: $\mathbf{q} = [\rho, \rho u, \rho i]^{\mathrm{T}}$. The system of differential equations to be considered is

$$\frac{\partial}{\partial t}\begin{bmatrix}\rho \\ \rho u \\ \rho i\end{bmatrix} + \frac{\partial}{\partial z}\begin{bmatrix}\rho u \\ u\,\rho u + P(\rho, i) \\ u[\rho i + P(\rho, i)]\end{bmatrix} = \begin{bmatrix}0 \\ \rho g(z) - \dfrac{K_{\mathrm{eff}}(\mathbf{q})}{2} u\,|\rho u| \\ \dot{Q}_{\mathrm{add}}(z, t)\end{bmatrix} \tag{2.3}$$

where $P(\rho, i)$ is the thermodynamic pressure of the fluid, $g(z)$ is an orientation specific gravitational constant as a function of position, $K_{\mathrm{eff}}(\mathbf{q})$ is an effective form/frictional loss factor, and $\dot{Q}_{\mathrm{add}}(z, t)$ is a specified heat source/sink to the system.

There are a number of assumptions in this model. Firstly, kinetic energy contributions in the third equation are assumed small compared to the internal energy terms and were, therefore, neglected. Similarly, energy dissipation due to frictional work is also taken to be negligible in the energy equation. In addition, the gradient of the viscous stress tensor in the momentum equation has been replaced by the algebraic effective loss term. The equation of state for $P(\rho, i)$ was chosen to be the IAPWS-95 formulation for water (see appendix A for details).

Equation 2.3 can also be viewed as a one-dimensional, one field conservation law. If so-called mixture properties are defined for all terms in the equation, it is said to be a HEM for flow. All components and phases of the fluid, while in reality separate, can be modeled as a single, averaged substance (homogeneous) possessing one temperature, velocity, etc. (equilibrium).

While a crude estimate to realistic flows, it is a considered a useful first-order approximation to how a thermal hydraulic system evolves.

To calculate the characteristic speeds of equation 2.3, the strong conservative form of equation 2.1 needs to be matched. Therefore, all of the primitive variables must be replaced by conserved ones in the formulation. Thus, equation 2.3 is written as

$$\frac{\partial}{\partial t}\begin{bmatrix}\rho\\ \rho u\\ \rho i\end{bmatrix}+\frac{\partial}{\partial z}\begin{bmatrix}\rho u\\ \dfrac{\rho u^2}{\rho}+P\left(\rho,\dfrac{\rho i}{\rho}\right)\\ \dfrac{\rho u}{\rho}\left[\rho i+P\left(\rho,\dfrac{\rho i}{\rho}\right)\right]\end{bmatrix}=\begin{bmatrix}0\\ \rho g(z)-\dfrac{K_{\text{eff}}(\mathbf{q})}{2}\dfrac{\rho u|\rho u|}{\rho}\\ \dot{Q}_{\text{add}}(z,t)\end{bmatrix} \tag{2.4}$$

The Jacobian of the flux function from this form with primitive variables is

$$\mathbb{J}_{\text{F}}=\begin{bmatrix}0 & 1 & 0\\ \dfrac{dP}{d\rho}-u^2 & 2\,u & \dfrac{1}{\rho}\dfrac{\partial P}{\partial i}\\ u\left(\dfrac{dP}{d\rho}-h\right) & h & u\left(1+\dfrac{1}{\rho}\dfrac{\partial P}{\partial i}\right)\end{bmatrix} \tag{2.5}$$

where the enthalpy h equals $i+P/\rho$ and the total derivative $dP/d\rho$ is explained in appendix B. The characteristic speeds of equation 2.5 are

$$\lambda_{\text{HEM}}=\begin{bmatrix}u\\ \left(1+\dfrac{1}{2\rho}\dfrac{\partial P}{\partial i}\right)u+\dfrac{1}{2\rho}\sqrt{4P(\rho,i)\dfrac{\partial P}{\partial i}+\left(u\dfrac{\partial P}{\partial i}\right)^2+4\rho^2\dfrac{\partial P}{\partial \rho}}\\ \left(1+\dfrac{1}{2\rho}\dfrac{\partial P}{\partial i}\right)u-\dfrac{1}{2\rho}\sqrt{4P(\rho,i)\dfrac{\partial P}{\partial i}+\left(u\dfrac{\partial P}{\partial i}\right)^2+4\rho^2\dfrac{\partial P}{\partial \rho}}\end{bmatrix} \tag{2.6}$$

The first characteristic speed of the system is the velocity u itself. Since this quantity refers to

something physical and measurable, it is often (and will be) referred to as the material speed. The other two speeds are a combination of the material speed and various thermophysical derivatives. These speeds will referred to as acoustic speeds because they simplify to $u \pm c$, where c is the sound speed of the fluid, if pressure was purely a function of density.

It is clear from equation 2.6 that the speed will always be purely real if the discriminant (the square root term) is always positive. The discriminant is a function of all three primitive variables of the system, but since the only term containing the velocity is squared, the lowest possible value of the discriminant will coincide with zero velocity. Explicit calculation of the remaining two terms with the equation of state over the rectangle $\rho = [0.005, 997]$ in kg/m^3 and $T = [290, 650]$ in K yielded a minimum discriminant of 0.224. Therefore, the speeds for HEM are always purely real.

2.1.2 Two-Phase

In transitioning from one-phase to two-phase, not much on the left-hand side of equation 2.3 changes, save the addition of a subscript to indicate what phase the quantity is representing and the concept of a volume fraction α. For the two fluid model, distinct phases are treated as separate partitions of a total volume with completely separate properties and only communicate through their shared interface. The fraction of the total volume that a given phase occupies is that phases's volume fraction; for example, if a liquid phase and gas phase occupy a single volume, there is a compatibility condition requiring $\alpha_\ell + \alpha_g = 1$. The big change in two-fluid formulations (and multiphase formulations in general) is the source functions on the right hand side of the conservation law.

Based on the conservative formulations of Ishii and Hibiki [19], the one dimensional conser-

vation laws for phase ϕ is

$$\frac{\partial}{\partial t}\begin{bmatrix}\alpha\rho_\phi\\ \alpha\rho u_\phi\\ \alpha\rho i_\phi\end{bmatrix}+\frac{\partial}{\partial z}\begin{bmatrix}\alpha\rho u_\phi\\ u_\phi\,\alpha\rho u_\phi+P(\rho_\phi,i_\phi)\\ u_\phi[\alpha\rho i_\phi+P(\rho_\phi,i_\phi)]\end{bmatrix}=\begin{bmatrix}\mathbb{M}_\phi\\ \alpha\rho_\phi g(z)-\dfrac{K_{\text{eff},\phi}(\mathbf{q})}{2}u_\phi\,|\alpha\rho u_\phi|+\mathbb{P}_\phi\\ \dot{Q}_{\text{add},\phi}(z,t)+\mathbb{E}_\phi\end{bmatrix} \tag{2.7}$$

where the conserved variables from the single phase case have the same definition times the phase's void fraction. The heat source and effective loss function have the same definition as before but possess corrections for proper phase apportionment. The new terms $\mathbb{M}_\phi$, $\mathbb{P}_\phi$, and $\mathbb{E}_\phi$ are mass, momentum, and energy sources, respectively, from the other phases (i.e., saturated liquid evaporating into the vapor phase or vapor condensing into the liquid). These terms, from a computational fluid dynamics perspective, do have mathematical definitions in Ishii's text. However, the one-dimensional system code perspective defines them with correlations for particular flow regimes. As currently formulated, equation 2.7's characteristic speeds are algebraically identical to the single phase model (except with twice as many speed, one set for each phase).

This equation set is also underdetermined: with two phases, there are eight unknowns (ρ_ℓ, ρ_g, ρu_ℓ, ρu_g, ρi_ℓ, ρi_g, α_ℓ, and α_g) and seven equations (six balance and one compatibility). A closed system that is commonly used is one that assumes equal pressure $P(\rho_\ell, i_\ell) = P(\rho_g, i_g)$. However, it has been mathematically proven that this system is ill-posed and may exhibit unphysical solutions [8]; although an assessment of RELAP5 (a systems code similar to MELCOR that uses this closure) concluded that the system is stable as long as the spatial mesh is not refined "too much" [37].

Full investigation of two-fluid closures, correlations, etc. is beyond the scope of this text and

left to future work.

2.2 Numerical Methods

Because equation 2.3 has no closed form solution as presented, numerical approximations are needed to observe the theoretical evolution of the system. First, a number of spatial discretizations will be discussed such that the system can be put into a so-called semi-discrete form. Then, time integration methods will be discussed.

2.2.1 Spatial Discretization

Before discussing the spatial discretizations, the end goals of the methods should be considered. Figure 2.1 shows the computational geometry to ultimately studied. Unlike a majority of the literature, the novelty of this research aims to tackle the stability of a non-simple, closed curve. Because the curve is non-simple, there are branch points which have more than one possible path, and the numerical methods must be amenable to this requirement. Also, the tank (the large volume topping the model) is open to atmosphere that allows for an unrecoverable loss of mass to the atmosphere, so the method should be able to allow for a flow of liquid from the system to an infinite sink.

Figure 2.1: Geometry required to model. The black, directed line is the non-simple, closed curve along which the conservation laws must be satisfied. The blue and red outlines denote the cooling and heating zones, respectively.

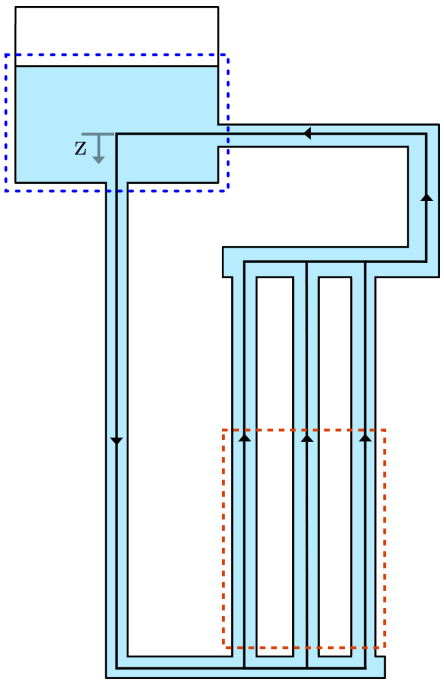

Collocated Nodal (Steady-state only)

The simplest (yet hardest) numerical example to begin with is the steady-state nodal method for a simply closed loop. Setting the time derivative of equation 2.3 to 0 yields

$$\frac{\partial}{\partial z}\begin{bmatrix} \rho u \\ u\,\rho u + P(\rho, i) \\ u[\rho i + P(\rho, i)] \end{bmatrix} = \begin{bmatrix} 0 \\ \rho g(z) - \dfrac{K_{\text{eff}}(\mathbf{q})}{2} u\,|\rho u| \\ \dot{Q}_{\text{add}}(z, t) \end{bmatrix} \tag{2.8}$$

and now, for ease of discussion and writing, the individual flux and source functions will be numbered:

$$\mathbf{F}(\mathbf{q};x) = \begin{bmatrix} F^1(\mathbf{q};z) \\ F^2(\mathbf{q};z) \\ F^3(\mathbf{q};z) \end{bmatrix} = \begin{bmatrix} \rho u \\ u\,\rho u + P(\rho,i) \\ u[\rho i + P(\rho,i)] \end{bmatrix} \tag{2.9}$$

$$\mathbf{S}(\mathbf{q},z) = \begin{bmatrix} S^1(\mathbf{q},z) \\ S^2(\mathbf{q},z) \\ S^3(\mathbf{q},z) \end{bmatrix} = \begin{bmatrix} 0 \\ \rho g(z) - \dfrac{K_{\text{eff}}(\mathbf{q})}{2} u\,|\rho u| \\ \dot{Q}_{\text{add}}(z,t) \end{bmatrix}, \tag{2.10}$$

Due to the nonlinearity of the problem, a numerical approximation to the solution of equation 2.8 will be attempted. Let $z^\dagger$ be a discrete partitioning of z into of the form

$$z_g = z_1 < z_2 < z_3 < ... < z_N < z_{N+1} = z_g,$$

where N is the number of approximate states. It is important to notice that since z, and therefore $z^\dagger$, is a closed circuit, z_1 and z_{N+1} map to the same location z_g. Integrating equation 2.8 over a given partition of $z^\dagger$, to be called a control volume, yields

$$\mathbf{F}(\mathbf{q};z_{i+1}) - \mathbf{F}(\mathbf{q};z_i) = \beta_i \mathbf{S}(\mathbf{q},z_i) + \beta_{i+1}\mathbf{S}(\mathbf{q},z_{i+1}) + \mathcal{O}(|z_{i+1} - z_i|^2), \tag{2.11}$$

where the source function has been integrated via the trapezoidal rule to yield a second order approximation to the system. While the true solution $\mathbf{q}$ exactly balances equation 2.11, if a discrete approximation $\mathbf{q}^\dagger$ is introduced and the trapezoidal error term ignored, the balance will more than likely be lost. This loss of balance results in a residual (error) function defined by

$$\mathrm{R}_i(\mathbf{q}^\dagger) = \left[\mathbf{F}(\mathbf{q}^\dagger;z_{i+1}) - \mathbf{F}(\mathbf{q}^\dagger;z_i)\right] - \left[\beta_i \mathbf{S}(\mathbf{q}^\dagger;z_i) + \beta_{i+1}\mathbf{S}(\mathbf{q}^\dagger;z_{i+1})\right]. \tag{2.12}$$

This equation leads to a system of nonlinear equations in $\mathbf{q}^\dagger$:

$$\begin{aligned}
\mathrm{R}_1(\mathbf{q}^\dagger) &= \left[\mathbf{F}(\mathbf{q}^\dagger; z_2) - \mathbf{F}(\mathbf{q}^\dagger; x_1)\right] - \left[\beta_1 \mathbf{S}(\mathbf{q}^\dagger; z_1) + \beta_2 \mathbf{S}(\mathbf{q}^\dagger; z_2)\right] \\
\mathrm{R}_2(\mathbf{q}^\dagger) &= \left[\mathbf{F}(\mathbf{q}^\dagger; z_3) - \mathbf{F}(\mathbf{q}^\dagger; x_2)\right] - \left[\beta_2 \mathbf{S}(\mathbf{q}^\dagger; z_2) + \beta_3 \mathbf{S}(\mathbf{q}^\dagger; z_3)\right] \\
&\vdots \\
\mathrm{R}_{N-1}(\mathbf{q}^\dagger) &= \left[\mathbf{F}(\mathbf{q}^\dagger; z_N) - \mathbf{F}(\mathbf{q}^\dagger; z_{N-1})\right] - \left[\beta_N \mathbf{S}(\mathbf{q}^\dagger; z_N) + \beta_{N-1} \mathbf{S}(\mathbf{q}^\dagger; z_{N-1})\right] \\
\mathrm{R}_N(\mathbf{q}^\dagger) &= \left[\mathbf{F}(\mathbf{q}^\dagger; z_1) - \mathbf{F}(\mathbf{q}^\dagger; z_N)\right] - \left[\beta_1 \mathbf{S}(\mathbf{q}^\dagger; z_1) + \beta_N \mathbf{S}(\mathbf{q}^\dagger; z_N)\right].
\end{aligned} \tag{2.13}$$

If a $\mathbf{q}^\dagger$ is found at each location in $z^\dagger$ such that each of the residuals is approximately 0, then $\mathbf{q}^\dagger$ is a solution to equation 2.12.

Equation 2.13 will now be written in a more succinct form to examine the structure of the system. Letting $\mathbf{F}^\dagger$ be the discrete, ordered flux function defined by

$$\mathbf{F}^\dagger = \mathbf{F}(\mathbf{q}^\dagger; z^\dagger) = \begin{bmatrix} [F^1(\mathbf{q}^\dagger; z_1) \dots F^1(\mathbf{q}^\dagger; z_N)]^T \\ [F^2(\mathbf{q}^\dagger; z_1) \dots F^2(\mathbf{q}^\dagger; z_N)]^T \\ [F^3(\mathbf{q}^\dagger; z_1) \dots F^3(\mathbf{q}^\dagger; z_N)]^T \end{bmatrix} \tag{2.14}$$

and $\mathbf{S}^\dagger$ be the discrete, ordered source function defined by

$$\mathbf{S}^\dagger = \mathbf{S}(\mathbf{q}^\dagger; z^\dagger) = \begin{bmatrix} [S^1(\mathbf{q}^\dagger, z_1) \dots S^1(\mathbf{q}^\dagger, z_N)]^T \\ [S^2(\mathbf{q}^\dagger, z_1) \dots S^2(\mathbf{q}^\dagger, z_N)]^T \\ [S^3(\mathbf{q}^\dagger, z_1) \dots S^3(\mathbf{q}^\dagger, z_N)]^T \end{bmatrix}, \tag{2.15}$$

equation 2.13 can be rewritten as

$$\mathrm{R}^\dagger = \mathbb{C}_F \mathbf{F}^\dagger - \mathbb{C}_S \mathbf{S}^\dagger. \tag{2.16}$$

The matrices $\mathbb{C}_F$ and $\mathbb{C}_S$ are the so-called system connectivity matrices as they describe how the individual control volumes of the whole system are linked to one another. Each of these connectivity matrices has the block structure

$$\mathbb{C}_* = \begin{bmatrix} \mathbf{C}_* & \mathbf{0} & \mathbf{0} \\ \mathbf{0} & \mathbf{C}_* & \mathbf{0} \\ \mathbf{0} & \mathbf{0} & \mathbf{C}_* \end{bmatrix}, \tag{2.17}$$

where $\mathbf{C}_*$ are law connectivity matrices, as they describe how a given conservation law is discretely linked in the system. The flux function's law connectivity matrix is $N \times N$ and has the sparse form

$$\mathbf{C}_F = \begin{bmatrix} -1 & +1 & & & \\ & -1 & +1 & & \\ & & \ddots & \ddots & \\ & & & -1 & +1 \\ +1 & & & & -1 \end{bmatrix}. \tag{2.18}$$

Similarly, the source function's law connectivity matrix has the sparse form

$$\mathbf{C}_S = \begin{bmatrix} \beta_1 & \beta_2 & & & \\ & \beta_2 & \beta_3 & & \\ & & \ddots & \ddots & \\ & & & \beta_{N-1} & \beta_N \\ \beta_1 & & & & \beta_N \end{bmatrix}. \tag{2.19}$$

It is noted that these submatrices are singular, due to a doubly reflective boundary conditions. That being the case, a solution not involving inversion of the matrices will be presented

in section 3.1.

Staggered Finite Volume

A problem with the previous section is not only the singularness of the connectivity matrices, but also that the method does not lend itself to arbitrary two-dimensional geometry per the problem to be investigated. Therefore, it is natural to switch over to a finite volume method that uses time integration to find possible steady-states. It will be noted that this section's title emphasizes "staggered" since there are collocated finite volume emthods. However, collocated schemes were not investigated here because it is very hard for them to properly conserve certain variables exactly [30].

A staggered mesh involves integrating the conservation laws over two different domains: control volumes and momentum cells. The control volumes typically hold all scalar quantities while the momentum cells serve as information propagators for the system with limited fluid residence time. Also, it is valuable to integrate the equations in three dimensions such that the gradients explicitly become surface integrals. Therefore, the equation's original form (equation 2.3) will be written with multidimensional derivatives (though this will be temporary and the flows are still, technically, one-dimensional).

Integrating the conservation of mass and energy equations over a closed, fixed volume Ω_k yields

$$\iiint_{\Omega_k} \frac{\partial}{\partial t} \begin{bmatrix} \rho \\ \rho i \end{bmatrix} \partial\Omega_k + \iiint_{\Omega_k} \nabla \begin{bmatrix} \rho u \\ u[\rho i + P(\rho, i)] \end{bmatrix} \partial\Omega_k = \iiint_{\Omega_k} \begin{bmatrix} 0 \\ \dot{Q}_{\text{add}}(z,t) \end{bmatrix} \partial\Omega_k \tag{2.20}$$

Because Ω_k is taken to be closed, the integral of the gradient can become a surface integral over Γ_k by the Divergence Theorem. Also, the volume average of some quantity ψ will be

defined as

$$\psi_{\mathrm{k}} = \frac{1}{\Omega_{\mathrm{k}}} \iiint_{\Omega_{\mathrm{k}}} \psi \partial\Omega_{\mathrm{k}}. \tag{2.21}$$

Equation 2.20 may now be re-written (with the time derivative alone on the left-hand side) as

$$\frac{\partial}{\partial t}\begin{bmatrix} \rho_{\mathrm{k}} \\ \rho i_{\mathrm{k}} \end{bmatrix} = -\frac{1}{\Omega_{\mathrm{k}}} \oiint_{\Gamma_{\mathrm{k}}} \begin{bmatrix} \rho u \\ u[\rho i + P(\rho, i)] \end{bmatrix} \hat{\mathbf{n}}\, \partial\Gamma_{\mathrm{k}} + \begin{bmatrix} 0 \\ \dot{Q}_{\mathrm{add,k}}(z,t) \end{bmatrix} \tag{2.22}$$

The $\hat{\mathbf{n}}$ (outward pointing is taken to be positive) in this equation says that material material flowing into material flowing into the volume is a source and material flowing out of the volume is a sink.

A similar procedure can be performed on the momentum equation over a volume Ω_{m} with surface Γ_{m} to yield

$$\frac{\partial \rho u_{\mathrm{m}}}{\partial t} = -\frac{1}{\Omega_{\mathrm{m}}} \oiint_{\Gamma_{\mathrm{m}}} u\, \rho u + P(\rho, i)\hat{\mathbf{n}}\, \partial\Gamma_{\mathrm{k}} + \frac{1}{\Omega_{\mathrm{m}}} \iiint_{\Omega_{\mathrm{m}}} \rho g(z) - \frac{K_{\mathrm{eff}}(\mathbf{q})}{2} u\, |\rho u|\, \partial\Omega_{\mathrm{m}} \tag{2.23}$$

In order to simplify equations 2.22 and 2.23 to fully algebraic in space, approximations must be made. The approximations made are

- The velocity distribution through all surfaces is uniform.
- The cross-sectional area through all momentum cells is constant.
- A momentum cell may only be connected to two control volumes called “from” and “to”.

The first two items allow the surface integrals to be written as summations over the number of non-zero flow in to and out of the control volumes/momentum cells. The last item allows

for the volume integral in equation 2.23 to be written as a line integral. The equations are now

$$\frac{\partial \rho_{\mathrm{k}}}{\partial t} = -\frac{1}{\Omega_{\mathrm{k}}} \sum \rho u_{\mathrm{k}} A_{\mathrm{k}} \tag{2.24a}$$

$$\frac{\partial \rho i_{\mathrm{k}}}{\partial t} = -\frac{1}{\Omega_{\mathrm{k}}} \sum u_d [\rho i_d + P(\rho_d, i_d)] A_{\mathrm{k}} + \dot{Q}_{\mathrm{add,k}}(z,t) \tag{2.24b}$$

$$\frac{\partial \rho u_{\mathrm{m}}}{\partial t} = -\frac{1}{\Omega_{\mathrm{m}}} \left[u\, \rho u |_{\mathrm{from}}^{\mathrm{to}} + P_{\mathrm{to}} - P_{\mathrm{from}} \right] A_{\mathrm{m}} + \frac{A_{\mathrm{m}}}{\Omega_{\mathrm{m}}} \int_{\mathrm{from}}^{\mathrm{to}} \left[\rho g(z) - \frac{K_{\mathrm{eff}}(\mathbf{q})}{2} u\, |\rho u| \right] \mathrm{d}s \tag{2.24c}$$

In this above form, so-called donor quantities ψ_{d} have been introduced. Donor quantities are a physical construct that conserves mass and energy exactly in the equations:

- If the momentum is a source to a volume, the donor quantity has the value of the control volume on the other side of the momentum cell.
- If the momentum is a sink to a volume, the donor quantity has the value of the control volume itself.

In the momentum equation, the pressure was evaluated explicitly at both ends of the momentum cell while the advective momentum term and source line were left to be defined by a model. Equation 2.24 is now a fully, semi-discrete ordinary differential equation. For an arbitrary number of control volumes K and momentum cells M, there is a solution vector $\mathbf{q} = [\rho_{\mathrm{K}}, \rho i_{\mathrm{K}}, \rho u_{\mathrm{M}}]^{\mathrm{T}}$ that always satisfies the ODE

$$\frac{\partial}{\partial t} \begin{bmatrix} \rho_{\mathrm{K}} \\ \rho i_{\mathrm{K}} \\ \rho u_{\mathrm{M}} \end{bmatrix} = \begin{bmatrix} n_{\rho}(\mathbf{q}) \\ n_{\rho i}(\mathbf{q}) \\ n_{\rho u}(\mathbf{q}) \end{bmatrix} \tag{2.25}$$

where the n functions are defined by equation 2.24 for the associated quantity. And more

simply

$$\frac{\partial \mathbf{q}}{\partial t} = N(\mathbf{q}) \tag{2.26}$$

This is the semi-discrete form to be considered.

2.2.2 Time Discretization

Time discretization is simply integration of some ODE from a known initial condition forward in time. There are many different methods for time integration. Some methods use information already known to calculate the time evolution (explicit methods) while others introduce an unknown state in the future and require the solution of a system to march forward in time (implicit methods).

Integrating equation 2.26 from t_0 to t_1 yields

$$\mathbf{q}(t_1) = \mathbf{q}(t_0) + \int_{t_0}^{t_1} N(\mathbf{q}) \mathrm{d}t \tag{2.27}$$

Because it is not known how $\mathbf{q}$ changes over the time period, an approximation to the integral must be made. If the integral is approximated by the old, known value of $\mathbf{q}$ times the time interval, the equation becomes

$$\mathbf{q}(t_1) = \mathbf{q}(t_0) + N(\mathbf{q}(t_0))(t_1 - t_0) \tag{2.28}$$

which is called the explicit Euler method. If, instead, the integral is approximated by the new, unknown value of $\mathbf{q}$ times the time interval, the equation becomes

$$\mathbf{q}(t_1) = \mathbf{q}(t_0) + N(\mathbf{q}(t_1))(t_1 - t_0) \tag{2.29}$$

Figure 2.2: Semilog plot of the acoustic speed versus material speed. The speeds vary over several orders of magnitude.

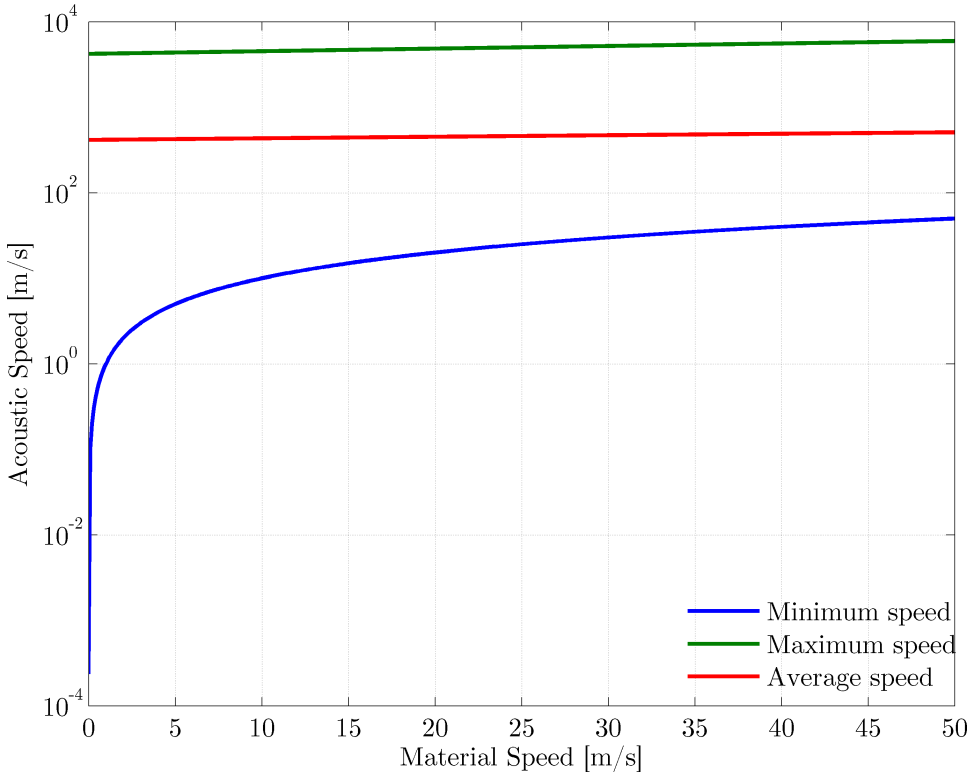

which is called the implicit Euler method. There are higher order methods for for explicit and implicit schemes, but they will not be explored here.

While the explicit Euler method is much simpler to perform, it was a limit to how large the time step $(t_1 - t_0)$ can be for the solution to be stable. Implicit Euler has no such limitation. The limitation on explicit Euler's time step is intimately connected to the maximum wave speed of the system being investigated. Going back to equation 2.6, the equations for the speed of the HEM system are known. A plot of the acoustic speeds versus the material speed using the rectangle $\rho = [0.005, 997]$ in kg/m^3 and $T = [290, 650]$ in K is shown in figure 2.2. It is shown that the acoustic waves can have a speed of several kilometers per second and will therefore dictate (i.e., extremely limit) the maximum time step for an explicit time march. In order to avoid this, among other reasons [12], implicit Euler will be explored in this and

future work.

2.3 Stability Analysis

Linear analysis of stability involves linearizing the governing, nonlinear equations. Chapter 2 discusses this in much more depth, but for now, it suffices to say that a small perturbation off of an assumed steady-state is introduced into the set of equations, the equations are then Taylor-expanded, and all terms beyond order one are neglected. The result is a set of linear, coupled partial differential equations. The equations are then integrated over some geometry to yield linear, coupled ordinary differential equations whose stability can be determined by numerous methods. One method is to to the Laplace transform of these equations to yield a set of algebraic equations which is typically reduced down to a single equation whose roots determine the system's stability. Another method is to solve for the eigenvalues of the coefficient matrix of the linear problem which determines the system's stability. Both methods are equivalent in that all of the roots' and eigenvalues' real parts must be negative for the system to be linearly stable; this is because negativity of the quantities guarantees exponential decay of the initial perturbation originally introduced into the system.

Chapter 3

Current Work

Much of the current work have been devoted to building the tools necessary to proceed to more complicated problems in the future. The thermodynamics package discussed in appendix A was a large effort in-itself. The transient solver for the computational geometry is still a work in progress. However, a steady-state solver for a simple, closed loop is completed and will be discussed.

3.1 Steady-state Solver

3.1.1 Description of the Algorithm

As discussed in section 2.2.1, the steady-state equations for a closed loop are singular and, therefore, not directly invertible. However, for a closed loop, the total pressure gradient is 0. Therefore, knowing that the density and internal energy of the starting point will be the same (meaning the same pressure), the loop can be integrated from end to end assuming a momentum. The pressure at the start (known) is then compared with the pressure at the end. The pressure at the end of the integration loop is a function of the initial momentum since it governs the frictional losses. If the end pressure is higher than the known state, there was not enough frictional pressure loss; the speed is increased and the integration is performed again. If the end pressure is lower than the known state, there was too much frictional pressure loss; the speed is deceased and the integration is performed again.

3.1.2 Test Problem

A simple natural circulation loop is shown in figure 3.1. The test problem is for single phase water with a pressure of 101325 Pa and temperature of 300 K. The power load is 10 kW added and removed. Because this is a single phase problem and water is nearly incompressible, the problem is approximately solvable by hand. Results for both the steady-state solver and the hand calculations are given in table 3.1.

While the problem is simple, it is a proof-of-concept that the solver works for single phase flow. Multiphase with HEM is currently being investigated.

Figure 3.1: A simple natural circulation loop for testing the steady-state solver. The blue and red outlines indicate cooling and heating zone, respectively. ; the total power added and removed is 10 kW. The green dot is the known state: pressure is 101325 Pa and temperature 300 K. The numbered dot coincide in the data listed in table 3.1.

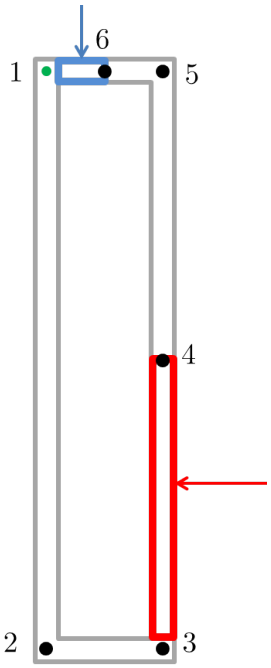

Table 3.1: Comparison between the written steady-state solver and a hand calculation for the same problem. The measurement points' location coincides with those in figure 3.1

Measure Point	**Pressure** [kPa]		**Temperature** [K]		**Density** [kg/m^3]	
	Solver	Hand	Solver	Hand	Solver	Hand
1	101325	101325	300.0	300	996.6	996.6
2	150192	150178	300.0	300	996.6	996.6
3	150190	150175	300.0	300	996.6	996.6
4	130640	130631	302.9	302.9	995.7	995.7
5	101327	101328	302.9	302.9	995.7	995.7
6	101326	101326	302.9	302.9	995.7	995.7

Appendix A

Thermophysical Properties

A.1 Equation of State

The equation of state used for the simulations is the International Association for the Properties of Water and Steam (IAPWS) Formulation 1995 for the Thermodynamic Properties of Ordinary Water Substance for General and Scientific Use (IAPWS-95) [17]. The specifics of the equation of state are discussed in the following section. Also, the procedure for back-calculating the temperature given a density and internal energy from the formulation is outlined since the conservation laws for the simulations evolve the internal energy based on mechanical balance but the equation of state uses temperature for explicit calculation of state properties.

A.1.1 IAPWS Formulation 1995

The IAPWS-95 is a fully non-ideal equation of state for water that uses on an empirical curve fit of the Helmholtz Free Energy potential A_{FE}. The natural variables of the potential are density ρ and temperature T, and the formulation uses a dimensionless density δ and a dimensionless temperature τ defined by

$$\delta = \frac{\rho}{\rho_{\text{c}}} \tag{A.1}$$

$$\tau = \frac{T_{\text{c}}}{T} \tag{A.2}$$

where ρ_c and T_c are, respectively, the critical point density and temperature of water. The dimensionless form of the potential is the fundamental basis of the IAPWS formulation and has the form

$$\frac{A_{FE}(\rho, T)}{RT} = \phi(\delta, \tau) = \phi^I(\delta, \tau) + \phi^R(\delta, \tau), \tag{A.3}$$

where ϕ^I is an ideal gas potential function, ϕ^R is a residual (i.e., non-ideal gas) potential function, and R is the specific gas constant of water. The actual functional form of $\phi(\delta, \tau)$ is cumbersome and will not be presented here (see [17] for a full description). Using this potential and its associated derivatives, all thermodynamic properties can be calculated for a given state. A select group of relationships between the potential and properties are presented in table A.1. The relationships are valid for the entire set of single phase states.

Table A.1: Select thermodynamic properties and associated dimensionless Helmholtz free energy relationships.

Property	Helmholtz Potential Relation
Pressure	$\frac{P}{R\rho_c T_c} = \left[1 + \delta\frac{\partial\phi^R}{\partial\delta}\right]\frac{\delta}{\tau}$
Internal Energy	$\frac{i}{RT_c} = \frac{\partial\phi}{\partial\tau}$
Entropy	$\frac{s}{R} = \tau\frac{\partial\phi}{\partial\tau} - \phi$
Enthalpy	$\frac{h}{RT_c} = \frac{1}{\tau}\left[1 + \tau\frac{\partial\phi}{\partial\tau} + \delta\frac{\partial\phi^R}{\partial\delta}\right]$

Additionally, the formulation permits calculation of saturated properties. Unlike the explicit, single phase equations above, saturated calculations involve a necessarily iterative procedure. Solving for a saturated condition involves leveraging the three equilibrium conditions of phase change: constant pressure, constant temperature, and phasic equality of Gibbs free energy. In terms of the non-dimensional Helmholtz free energy function $\phi(\delta, \tau)$, these equilibrium

conditions form a system of equations that must be simultaneously satisfied:

$$\frac{P_{\text{sat}}}{R\rho_{\text{c}}T_{\text{c}}} = \left[1 + \delta_\ell \frac{\partial \phi^{\text{R}}}{\partial \delta}(\delta_\ell, \tau_{\text{sat}})\right] \frac{\delta_\ell}{\tau_{\text{sat}}} \tag{A.4a}$$

$$\frac{P_{\text{sat}}}{R\rho_{\text{c}}T_{\text{c}}} = \left[1 + \delta_g \frac{\partial \phi^{\text{R}}}{\partial \delta}(\delta_g, \tau_{\text{sat}})\right] \frac{\delta_g}{\tau_{\text{sat}}} \tag{A.4b}$$

$$\frac{P_{\text{sat}}}{R\rho_{\text{c}}T_{\text{c}}} = \left[\text{Ln}\left(\frac{\delta_\ell}{\delta_g}\right) + \phi^{\text{R}}(\delta_\ell, \tau_{\text{sat}}) - \phi^{\text{R}}(\delta_g, \tau_{\text{sat}})\right] \frac{\delta_\ell \delta_g}{\tau_{\text{sat}}(\delta_\ell - \delta_g)}. \tag{A.4c}$$

Equations A.4a and A.4b arise from the definition of pressure in terms of the Helmholtz free energy and the pressure equality of the functions given the saturated liquid density ρ_ℓ and gas density ρ_g at the saturation temperature. Equation A.4c is the Maxwell construction (i.e., equal area rule) of the Gibbs free energy equivalence ([13]). The above system consists of three equations and four unknowns: P_{sat}, τ_{sat}, δ_ℓ, and δ_g; therefore, the system can be solved once one of the saturation values is specified. A pressure-volume diagram is shown in figure A.1 calculated from an implementation of the IAPWS-95 formulation.

A.1.2 Back Calculation of Temperature

Temperature is a very powerful state variable because it is a directly measurable quantity that provides a qualitative measurement of a fluid's internal energy. However, in the balance equations equation 2.3, density and internal energy are the variables that are mechanically balanced, completely independent of thermodynamics. As such, it is most natural to update the thermodynamic and transport quantities with the mechanically specified density and internal energy to have a consistent evolution system. Furthermore, since density and internal energy are defined and independent in the two-phase region (unlike pressure and temperature), the time evolution may lead to mixture quantities.

The solution procedure chosen relies on one key fact about the relationship between internal

Figure A.1: Pressure versus specific volume with several isotherms. The gray line denotes the phase coexistence curve.

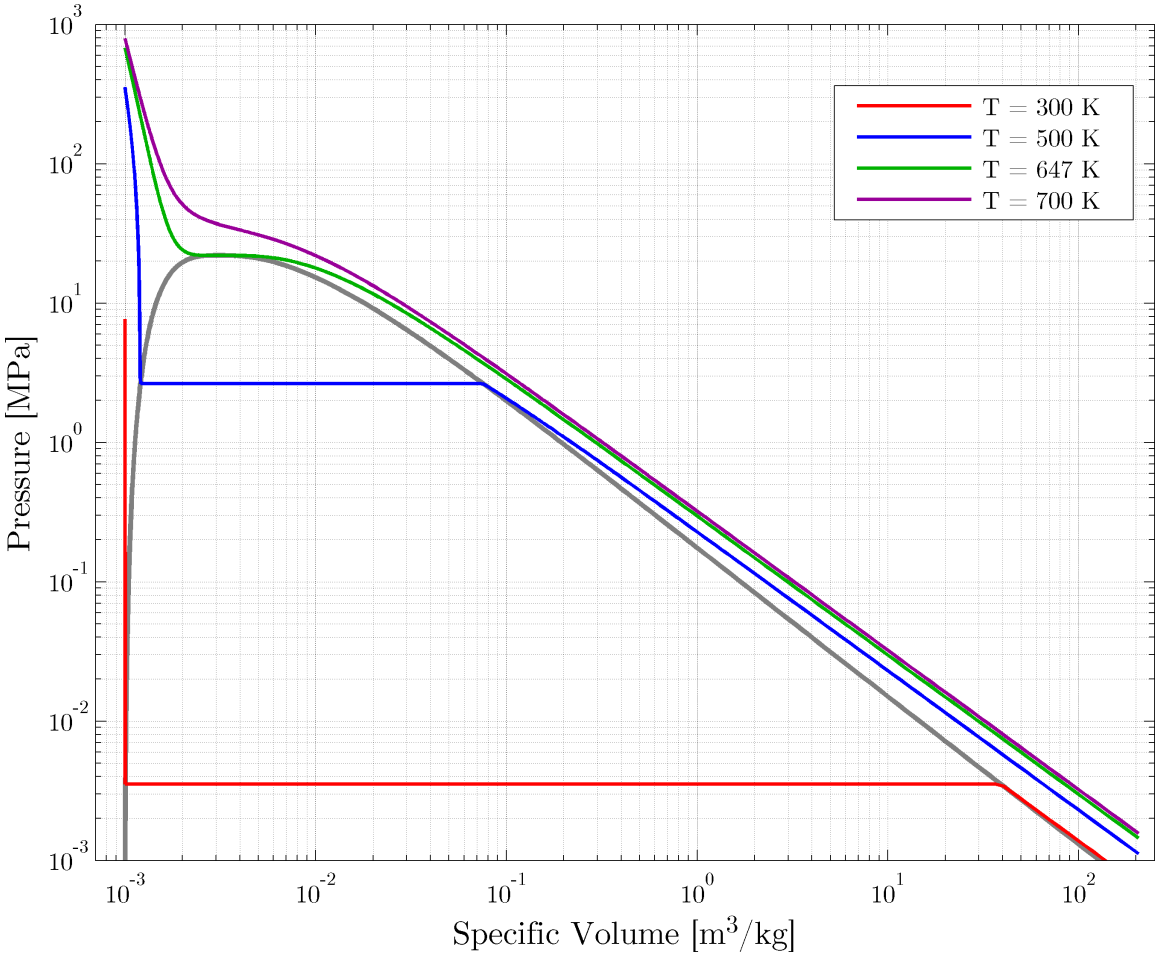

energy and temperature: along an arbitrary isochore, internal energy is an injective, monotonic function of temperature. One result of this fact is that a single phase internal energy will always be higher than its saturation value at the current density; this allows for an explicit determination of one- or two-phase conditions (see figure A.2 for a phase diagram). Another result is that root-finding procedures can be readily used to calculate the temperature for a state defined by density and internal energy. In the single phase region with a given guess value, the dimensionless temperature is calculated by driving the following residual formula to zero through Newton's method:

$$R(\tau) = \frac{\partial \phi}{\partial \tau}(\delta, \tau) - \frac{i}{RT_{\mathrm{c}}}. \tag{A.5}$$

For the two-phase region, the situation is a bit more complicated since the mixture internal energy must be calculated at every temperature update and $\partial\phi/\partial\tau$ approximated numerically since no closed form exists. The full algorithm is outlined below. Once the temperature has been calculated, all other properties can be directly solved for using the natural variables of the Helmholtz potential.

Algorithm: Temperature Back Calculation

Input: A known dimensionless density δ and internal energy i.
Output: Corresponding dimensionless temperature τ.

$i_{\text{sat}} = \text{GetSaturationInternalEnergy}(\delta)$
if $i > i_{sat}$ **then**
  % Single phase solve
  $\tau = \tau_{\text{guess}}$
  $d\tau = \text{Inf}$
  while $\text{Abs}(d\tau) > \varepsilon$ **do**
    $d\tau = -\,\text{R}_{\text{one}}(\tau)/\,\text{R}'_{\text{one}}(\tau)$
    $\tau = \tau + d\tau$
  end
else
  % Two-phase solve
  $\tau = \tau_{\text{guess}}$
  $d\tau = \text{Inf}$
  while $\text{Abs}(d\tau) > \varepsilon$ **do**
    $[P_{\text{sat}}, \delta_\ell, \delta_g] = \text{GetSaturationProperties}(\tau)$
    $d\tau = -\,\text{R}_{\text{two}}(\tau)/\,\text{R}'_{\text{two}}(\tau)$
    $\tau = \tau + d\tau$
  end
end

Above is an algorithmic outline of the temperature back calculation. The functions GetSaturationInternalEnergy() and GetSaturationProperties() rely on solving equation A.4 through another Newton method. The residual R_{one} is the same as equation A.5 while R_{two} calculates the mixture internal energy at the current τ iterant and the approximates the derivative in the vapor dome (since there is no closed form).

Figure A.2: Internal energy versus density with an arbitrary isochore. From the shape of the vapor dome in ρ-i space, it is clear that the saturation internal energy is always less than the single phase along an isochore.

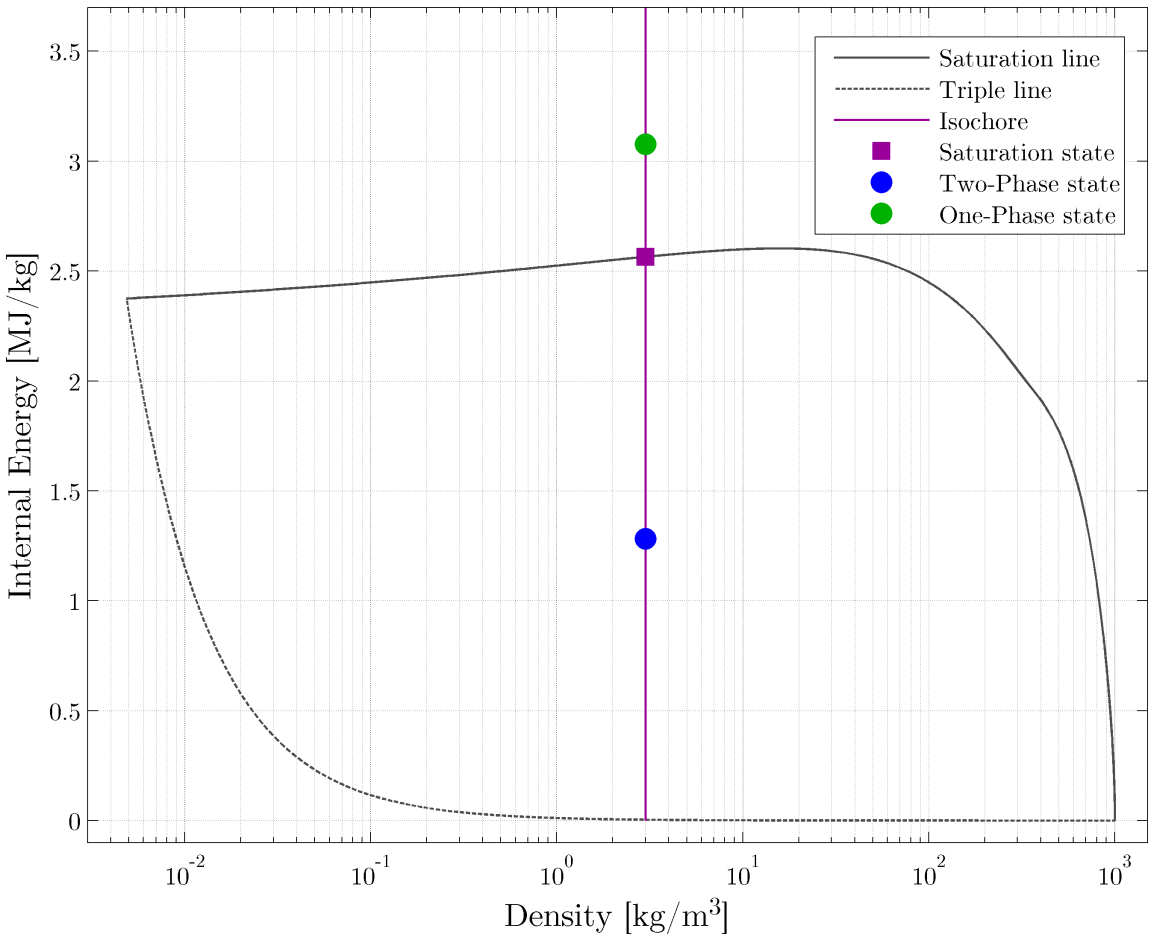

A.2 Transport Properties

Thermal conductivity κ and dynamic viscosity μ are transport properties and have no direct relation to thermodynamic potentials. However, the IAPWS has curve fits that are functions of density and temperature and are meant to be used in conjunction with the IAPWS-95 equation of state [16, 18].

Appendix B

Total Derivatives

In chapter 2, a function for the thermodynamic pressure was presented that was explicitly a function of the density ρ and the conservative internal energy i/ρ. For that function, the total derivative with respect to the conserved variable ρ is

$$\frac{dP}{d\rho} = \frac{\partial P}{\partial \rho} - \frac{\rho i}{\rho^2}\frac{\partial P}{\partial i} \tag{B.1}$$

$$= \frac{\partial P}{\partial \rho} - \frac{i}{\rho}\frac{\partial P}{\partial i} \tag{B.2}$$

and with respect to the conserved variable ρi is

$$\frac{dP}{d(\rho i)} = \frac{1}{\rho}\frac{\partial P}{\partial i} \tag{B.3}$$

However, since the equation of state presented in section A.1 is explicitly a function of density and temperature, the derivatives that arise from Jacobians have a more complicated form. The relationship between a thermodynamic function $\psi(\rho,i)$ and $\psi_{\text{EOS}}(\rho,T)$ is, in conservative form,

$$\psi\left(\rho, \frac{\rho i}{\rho}\right) = \psi_{\text{EOS}}\left[\rho, T\left(\rho, \frac{\rho i}{\rho}\right)\right]. \tag{B.4}$$

From this equation, the total derivative with respect to ρ is

$$\frac{d\psi}{d\rho} = \frac{\partial \psi_{\text{EOS}}}{\partial \rho} + \frac{\partial \psi_{\text{EOS}}}{\partial T}\left[\frac{\partial T}{\partial \rho}\right)_i - \frac{i}{\rho}\frac{\partial T}{\partial i}\Big)_\rho\Bigg] \tag{B.5}$$

and with respect to ρi is

$$\frac{d\psi}{d(\rho i)} = \frac{1}{\rho}\frac{\partial \psi_{\text{EOS}}}{\partial T}\frac{\partial T}{\partial i}\Bigg)_{\rho} \tag{B.6}$$

where the constancy of properties has been emphasized with purpose. The derivative of the temperature with respect to density in equation B.5 seems unwieldy since the IAPWS takes those properites to be independent; however, the requirement that the derivative is taken along a line of constant internal energy admits a solution. By the Implicit function theorem, the derivative of temperature with respect to density holding some thermodynamic property ψ constant is

$$\frac{\partial T}{\partial \rho}\Bigg)_{\psi} = -\frac{\partial \psi}{\partial \rho}\Bigg)_{T}\left[\frac{\partial \psi}{\partial T}\Bigg)_{\rho}\right]^{-1} \tag{B.7}$$

provided that $\partial\psi/\partial T$ is non-zero and $\psi(\rho, T)$ has (at least) a continuous first derivative at the evaluation state [14]. By the Inverse function theorem, the derivative of temperature with respect to some thermodynamic property ψ is

$$\frac{\partial T}{\partial \psi}\Bigg)_{\rho} = \left[\frac{\partial \psi}{\partial T}\Bigg)_{\rho}\right]^{-1}. \tag{B.8}$$

provided that $\partial\psi/\partial T$ is non-zero and $\psi(\rho, T)$ has (at least) a continuous first derivative at the evaluation state [14]. Equation B.8 is useful since $\partial\psi/\partial T$ is directly calculable from the IAWPS-95 equation of state in the single phase region (two-phase conditions require a numeric approximation to the derivative).

For the range of states considered in this work, the requirement that all the properties vary with temperature (i.e., non-zero derivative) is easily found to be valid. Concerning the smoothness condition, while the IAPWS-95 implementation is by-construction smooth in the single phase region, it is *not* continuously differentiable at the two-phase boundary (only continuous) with either quality or void fraction weighting. Therefore, with a homogeneous

equilibrium flow model, the inverse and implicit function theorems are inapplicable without some exception used at the boundary. That exception has been made in the implementation: for a purely saturated state, the derivatives used are those of the single phase fluid.

Lastly, it will be noted that while conservation of density through ρ is universal, conservation of energy through ρi is an approximation. The approximation of conservation through ρi ignores kinetic and potential energy of the fluid. While potential energy is usually included as a source term only, kinetic energy is commonly added to the internal energy to form the total energy of the system. If the energy equation was required to explicitly conserve thermal and kinetic energy, the conserved property would be defined as

$$\mathscr{e} = \rho i + \frac{1}{2}\frac{\rho u^2}{\rho} \tag{B.9}$$

and internal energy would have the form

$$i = \frac{\mathscr{e}}{\rho} - \frac{1}{2}\left(\frac{\rho u}{\rho}\right)^2. \tag{B.10}$$

Thus, in this formulation, the thermodynamic derivatives would have a momentum dependence in any Jacobian containing them. However, the current work does not explicitly conserve kinetic energy, and exploration of this form is left to future work.

Bibliography

[1] J. Achard, D. Drew, R. Lahey, Analysis of nonlinear density-wave oscillations in boiling channels., Journal of Fluid Mechanics 155 (1985) 213232.

[2] M. Aritomi, J. H. Chiang, M. Mori, Geysering in parallel boiling channels, Nuclear Engineering and Design 141 (12) (1993) 111–121.
URL http://www.sciencedirect.com/science/article/pii/002954939390096R

[3] M. Aritomi, J. H. Chiang, T. Nakahashi, M. Wataru, M. Mori, Fundamental study on thermo-hydraulics during start-up in natural circulation boiling water reactors, (I), Journal of Nuclear Science and Technology 29 (7) (1992) 631–641.
URL http://www.tandfonline.com/doi/abs/10.1080/18811248.1992.9731576

[4] Bechtel National, Inc., 450 MWt reactor cavity cooling system design description, DOE-HTGR-90016, Revision 0 (Nov. 1993).

[5] J. Bour, A. Mihaila, The oscillatory behavior of heated channels, An analysis of the density effect. Part I: the mechanism (nonlinear analysis). Centre d'Etudes Nucleaires de Grenoble, Report CEA 3049.

[6] J. Boure, A. Bergles, L. Tong, Review of two-phase flow instability, Nuclear Engineering and Design 25 (2) (1973) 165–192.
URL http://www.sciencedirect.com/science/article/pii/0029549373900435

[7] F. D'Auria, G. Galassi, Characterization of instabilities during two-phase natural circulation in typical PWR conditions, Experimental Thermal and Fluid Science 3 (6) (1990) 641–650.
URL http://www.sciencedirect.com/science/article/pii/089417779090081H

[8] T. Dinh, R. Nourgaliev, T. Theofanous, Understanding the ill-posed two-fluid model, proceedings of the 10th International Topical Meeting on Nuclear Reactor Thermal-Hydraulics (NURETH03) (2003).

[9] G. V. Durga Prasad, M. Pandey, M. S. Kalra, Review of research on flow instabilities in natural circulation boiling systems, Progress in Nuclear Energy 49 (6) (2007) 429–451.
URL http://www.sciencedirect.com/science/article/pii/S0149197007000480

[10] General Atomics, Gas turbine-modular helium reactor (GT-MHR) conceptual design description report, 910720 Revision 1 (Jul. 1996).
URL http://pbadupws.nrc.gov/docs/ML0224/ML022470306.html

[11] S. M. Ghiaasiaan, Two-Phase Flow, Boiling, and Condensation: In Conventional and Miniature Systems, 1st ed., Cambridge University Press, 2007.

[12] S. Gottlieb, D. I. Ketcheson, C.-W. Shu, High order strong stability preserving time discretizations, Journal of Scientific Computing 38 (3) (2009) 251–289.
URL http://link.springer.com/article/10.1007/s10915-008-9239-z

[13] H. Gould, J. Tobochnik, The chemical potential and phase equilibria, in: Statistical and Thermal Physics: With Computer Applications, Princeton University Press, 2010, pp. 357–388.
URL http://stp.clarku.edu/notes/chap7.pdf

[14] M. Greenberg, Advanced Engineering Mathematics, 2nd ed., Pearson, 1998.

[15] S. Guanghui, J. Dounan, K. Fukuda, G. Yujun, Theoretical and experimental study on density wave oscillation of two-phase natural circulation of low equilibrium quality, Nuclear Engineering and Design 215 (3) (2002) 187–198.
URL http://www.sciencedirect.com/science/article/pii/S0029549301004563

[16] IAPWS, Release on the IAPWS formulation 2008 for the viscosity of ordinary water substance (Sep. 2008).
URL http://www.iapws.org/relguide/viscosity.htm

[17] IAPWS, Revised release on the IAPWS formulation 1995 for the thermodynamic properties of ordinary water substance for general and scientific use (Sep. 2009).
URL http://www.iapws.org/relguide/IAPWS-95.htm

[18] IAPWS, Release on the IAPWS formulation 2011 for the thermal conductivity of ordinary water substance (Sep. 2011).
URL http://www.iapws.org/relguide/ThCond.htm

[19] M. Ishii, T. Hibiki, Thermo-Fluid Dynamics of Two-Phase Flow, Springer, 2011.

[20] R. W. Johnson, The Handbook of Fluid Dynamics, 1st ed., Springer, 1998.

[21] S. Kakac, B. Bon, A review of two-phase flow dynamic instabilities in tube boiling systems, International Journal of Heat and Mass Transfer 51 (34) (2008) 399–433.
URL http://www.sciencedirect.com/science/article/pii/S0017931007005959

[22] A. Knaani, Y. Zvirin, Bifurcation phenomena in two-phase natural circulation, International Journal of Multiphase Flow 19 (6) (1993) 1129–1151.
URL http://www.sciencedirect.com/science/article/pii/0301932293900815

[23] J. D. Lee, C. Pan, Nonlinear analysis for a double-channel two-phase natural circulation loop under low-pressure conditions, Annals of Nuclear Energy 32 (3) (2005) 299–329.
URL http://www.sciencedirect.com/science/article/pii/S030645490400204X

[24] S. Y. Lee, M. Ishii, Thermally induced flow oscillation in vertical two-phase natural circulation loop, Nuclear Engineering and Design 122 (13) (1990) 119–132.
URL http://www.sciencedirect.com/science/article/pii/0029549390902018

[25] S. Y. Lee, D. W. Lee, Linear analysis of flow instabilities in an open two-phase natural circulation loop, Nuclear Engineering and Design 128 (3) (1991) 317–330.
URL http://www.sciencedirect.com/science/article/pii/002954939190169I

[26] R. J. LeVeque, Finite Volume Methods for Hyperbolic Problems, 1st ed., Cambridge University Press, 2002.

[27] C. P. Marcel, M. Rohde, T. Van Der Hagen, Experimental and numerical investigations on flashing-induced instabilities in a single channel, Experimental Thermal and Fluid Science 33 (8) (2009) 1197–1208.
URL http://www.sciencedirect.com/science/article/pii/S0894177709001204

[28] C. P. Marcel, M. Rohde, T. Van Der Hagen, Experimental investigations on flashing-induced instabilities in one and two-parallel channels: A comparative study, Experimental Thermal and Fluid Science 34 (7) (2010) 879–892.
URL http://www.sciencedirect.com/science/article/pii/S0894177710000269

[29] A. Mills, Heat and Mass Transfer, Har/Dsk ed., CRC Press, 1994.

[30] Y. Morinishi, T. Lund, O. Vasilyev, P. Moin, Fully conservative higher order finite difference schemes for incompressible flow, Journal of Computational Physics 143 (1) (1998) 90–124.
URL http://www.sciencedirect.com/science/article/pii/S0021999198959629

[31] A. Nayak, P. Dubey, D. Chavan, P. Vijayan, Study on the stability behaviour of two-phase natural circulation systems using a four-equation drift flux model, Nuclear Engineering and Design 237 (4) (2007) 386–398.
URL http://www.sciencedirect.com/science/article/pii/S0029549306003876

[32] A. K. Nayak, P. K. Vijayan, Flow instabilities in boiling two-phase natural circulation systems: A review, Science and Technology of Nuclear Installations 2008 (2008) 1–15.
URL http://www.hindawi.com/journals/stni/2008/573192/abs/

[33] L. Neal, S. Zivi, R. Wright, The mechanisms of hydrodynamic instabilities in boiling channel, EURATOM Report, Pro-ceedings of Symposium on Two-Phase Flow Dynamics, Eindhoven (1967).

[34] Nuclear Regulatory Comminission, U.S. nuclear regulatory commission regulations: Title 10, code of federal regulations (Aug. 2007).
URL http://www.nrc.gov/reading-rm/doc-collections/cfr/

[35] Sandia National Laboratories, MELCOR computer code manuals: Reference manual, version 2.1 (2011).

[36] A. Satoh, K. Okamoto, H. Madarame, Instability of single-phase natural circulation under double loop system, Chaos, Solitons & Fractals 9 (9) (1998) 1575–1585.
URL http://www.sciencedirect.com/science/article/pii/S0960077997001173

[37] A. Shieh, V. Ransom, R. Krishnamurthy, RELAP5/MOD3 code manual: Validation of numerical techniques in RELAP5/MOD3, volume 6 (Aug. 1994).
URL http://pbadupws.nrc.gov/docs/ML1103/ML110330272.pdf

[38] J. Thome, Chapter 12: Two-phase flow patterns, in: Wolverine engineering data book III, Wolverine Tube Inc, 2004, pp. 12–1–12–34.
URL http://www.wlv.com/products/databook/db3/data/db3ch12.pdf

[39] L. S. Tong, Y. S. Tang, Boiling Heat Transfer And Two-Phase Flow, 2nd ed., CRC Press, 1997.

[40] G. B. Wallis, J. H. Heasley, Oscillations in two-phase flow systems, Journal of Heat Transfer 83 (3) (1961) 363.
URL http://link.aip.org/link/JHTRAO/v83/i3/p363/s1&Agg=doi

[41] P. Welander, On the oscillatory instability of a differentially heated fluid loop, J. Fluid Mech 29 (1) (1967) 1730.

[42] G. Yun, G. Su, J. Wang, W. Tian, S. Qiu, D. Jia, J. Zhang, Two-phase instability analysis in natural circulation loops of china advanced research reactor, Annals of Nuclear Energy 32 (4) (2005) 379–397.
URL http://www.sciencedirect.com/science/article/pii/S030645490400218X

[43] Y. Zvirin, R. Greif, Transient behavior of natural circulation loops: Two vertical branches with point heat source and sink, International Journal of Heat and Mass Transfer 22 (4) (1979) 499–504.
URL http://www.sciencedirect.com/science/article/pii/001793107990053X